Decadal shifts of coastal microphytoplankton communities in a semi-enclosed bay of NW Mediterranean Sea subjected to multiple stresses

B. Serranito, Jean-Louis Jamet, N Rossi , Dominique Jamet

Contents lists available at ScienceDirect

Estuarine, Coastal and Shelf Science

journal homepage: www.elsevier.com

Decadal shifts of coastal microphytoplankton communities in a semi-enclosed bay of NW Mediterranean Sea subjected to multiple stresses

B. Serranito [1, 2, *], J.-L. Jamet [1], N. Rossi [1], D. Jamet [1]

[1] Université de Toulon, Mediterranean Institute of Oceanology (MIO), UM 110, CNRS/INSU/IRD, Equipe EMBIO, CS 60584, 83041, Toulon Cedex 9, France
[2] Université de Limoges, Laboratoire PEREINE, INRA/IRSTEA, 87032, Limoges, France

ARTICLE INFO

ABSTRACT

Long-term evolution of microphytoplankton communities remains poorly studied in anthropized coastal zones submitted to multiple stressors. Here, we investigate decadal (2005–2017) microphytoplankton community changes, focusing on abundance and biovolume of major taxa related to both local abiotic conditions (rainfall rate, temperature and salinity) and regional convection events (wintering deep mixing) in the highly urbanized and semi-enclosed Toulon Bay (NW Mediterranean Sea). Results showed that persistent variations in local rainfall regime were followed by major changes in microphytoplankton community composition. Wet period (P_2) (increase of wintering precipitations observed between late 2008 and early 2015) was associated to an increase of large heterotrophic dinoflagellates and disappearance of dominant diatom taxa, while dry periods (2005–2008 (P_1) and 2015–2017 (P_3)) promoted diatoms, microflagellates and small mixotrophic/heterotrophic dinoflagellates including potentially toxic species. Concomitance between intense deep mixing events, reported in open Ligurian Basin (particularly during winters 2005 and 2006) and higher values in the total microphytoplankton abundance and in spring diatom abundance regardless of rainfall conditions, presents this meso-scale process as the main fertilization mechanism in Toulon Bay. Although no change was detected in the chlorophyll *a* concentration during the 2006–2017 period, its trend was negatively correlated to the total microphytoplankton abundance. This negative relation as well as a change of size in dinoflagellates suggested a shift in the primary producer nature, from large autotrophic cells (diatoms and microflagellates) to smaller ones, driven by a runoff intensification. Finally, different communities composition were observed during both dry periods (*i.e.* diatoms-dominated and autotrophic microflagellate-dominated communities during P_1 and P_3, respectively), suggesting another environmental driver of change for phytoplankton communities of this coastal ecosystem.

1. Introduction

Microphytoplankton defining photoautotrophic plankton range between 20 and 200 μm (Sieburth et al., 1978) is a master piece of marine systems as it represents one of the main component of primary production (Uitz et al., 2012). Shaping the most efficient carbon transfer along the trophic web (Cushing, 1989), microphytoplankton also plays a major role in biochemical cycles such as atmospheric carbon sequestration and export (Basu and Mackey, 2018) or in most of HAB (Harmful Algal bloom) events (Vila and Maso, 2005). Thus, many studies have predicted that changes in microphytoplankton communities and abundance could have large impacts on trophic web structure (Chivers et al., 2017; D'Alelio et al., 2015; Stibor et al., 2004), biochemical cycles (Guidi et al., 2016; Litchman et al., 2007; Wang et al., 2018) as well as water quality (Cloern and Dufford, 2005).

This latest concern affects particularly coastal zone which provides among the most of ecological services to human being (Costanza et al., 2014; de Groot et al., 2012). Coastal systems located at the sea-land interface, are subjected to multiple perturbations (Tett et al., 2007), related to climate variability and anthropogenic pressure such as nutrient enrichment from river runoff (Cloern et al., 2016). In this context, numerous works have highlighted the relevance of microphytoplankton communities as an indicator for the assessment of "good environmental status" (GES) of EU marine waters required by the Water Framework Directive (WFD: 2000/60/EC) (Devlin et al., 2007; Jaanus et al., 2009; Tett et al., 2013, 2008).

For a long time, these issues have increased interest in microphytoplankton monitoring in relation to variations of environmental condi-

* Corresponding authorUniversité de Toulon, Mediterranean Institute of Oceanology (MIO), UM 110, CNRS/INSU/IRD, Equipe EMBIO, CS 60584, 83041, Toulon cedex 9, France
Email address: serranitobruno@gmail.com (B. Serranito)

https://doi.org/10.1016/j.ecss.2019.04.049
Received 26 November 2018; Received in revised form 15 April 2019; Accepted 29 April 2019
Available online xxx
0272-7714/

tions in order to determine mechanisms driving and structuring communities at annual and interannual scales. Although microphytoplankton was mainly composed by diatoms (*Ochrophyta;* Cavalier-Smith, 1995) and dinoflagellates (*Myzozoa;* Cavalier-Smith and Chao, 2004), the high taxonomical and morphological diversity (Naselli-Flores et al., 2007) already mentioned by the Margalef "plankton paradox" (Margalef, 1963), remains a hindrance to the assessment of these concerns. In application of the guild concept (Root, 1967), trait-based approaches using measurable properties from organisms (McGill et al., 2006) are nowadays currently used to summarize the functional diversity of phytoplankton communities. Cell size has been considered as a "master trait" (Weithoff and Beisner, 2019), as it conditioned many physiological and ecological functions such as metabolic rate (López-Urrutia et al., 2006), nutrient intakes (Grover, 1989; Marañón, 2015) or trophic interactions (Barton et al., 2013; Hansen et al., 1994). Early on, size-based approaches succeed to describe important succession and distribution patterns related to environment such as the classical diatoms to dinoflagellates phenological succession in temperate coastal systems (Margalef, 1978) or the description of community niches along environmental gradients (Smayda and Reynolds, 2003, 2001). Species-specific biovolumes are particularly useful to describe mixed communities exhibiting a wide range of complex shapes (Ignatiades, 2015), reflecting species adaptations and strategies under diverse environmental and nutrient conditions for diatoms (Kemp and Villareal, 2018; Smayda and Reynolds, 2003) or dinoflagellates (Reynolds, 2006). For instance, it was also shown that cell sizes and shapes determines the prey nature for mixotrophic and heterotrophic dinoflagellates (Jeong et al., 2010). Such features play a crucial role on marine ecosystems impacting trophic web efficiency (Ward and Follows, 2016) but still remain poorly considered in phytoplankton dynamic studies (Flynn et al., 2013; Mitra and Flynn, 2010).

For decades, chlorophyll *a* concentration (and derived parameters) was widely used in long-term phytoplankton studies as a proxy of phytoplankton biomass (Cullen et al., 2002), because it allows to study homogenously primary production at large spatio-temporal scales (O'Reilly et al., 1998). Although these methods have shown significant advances in the recognition of functional types (Nair et al., 2008) or size classes (Brewin et al., 2011), it only roughly describes the size structure from phytoplankton communities (Boyce et al., 2015). Thus, long-term time series from stations remain critical and powerful tools for describing and studying high-resolution community variability related to environmental forcings (Adolf et al., 2006; Ducklow et al., 2009; Harding et al., 2016; Olli et al., 2008). However, the high cost associated with the establishment and the maintenance of stationary long-term time series may explain the limited number of coastal system monitoring at global scale (Smetacek and Cloern, 2008). Mediterranean sea which was designated as a hotspot to survey the impact of environmental variations on marine ecosystems, is unfortunately particularly subject to low monitoring effort (Mazzocchi et al., 2007).

As a result, only few investigations have attempt to characterize interannual variations of coastal microphytoplankton communities (Garrido et al., 2014) unlike to other plankton compartments such as zooplankton (Siokou-Frangou et al., 2010). Finally, due to an additional effort required, cell size is rarely considered in these long-term microphytoplankton community studies which mainly focus on abundance and taxonomic diversity which make difficult the comparison between ecosystems (Vadrucci et al., 2007). This lack of knowledge has, for instance led to promote chlorophyll *a* concentration as the only parameter to assess water coastal quality in Mediterranean GIG (Geographical Intercalibration Group) country members (Höglander et al., 2013) while some other basins such as North Sea (Devlin et al., 2007) or Baltic Sea (Höglander et al., 2013; Tett et al., 2008) focused on shift in functional groups as Biological Quality Element (BQE).

From remote sensing of chlorophyll *a* concentrations, the Ligurian Basin (NW Mediterranean sea) has been identified as a "intermittent" and a "blooming" ecoregion (d'Ortenzio and Ribera d'Alcalà, 2009). This category defines Mediteranean areas displaying intense spring blooms fueled by wintering deep mixing events (Coppola et al., 2018; Marty and Chiavérini, 2010). During the 2000s, three main events related to the deepening of the MLD (Mix Layer Depth) have been reported at the DYFAMED point (Ligurian Sea): winters 2005 and 2013 (D'Ortenzio et al., 2014; Coppola et al., 2018) and a particularly intense one occurring in winter 2006 (Coppola et al., 2018; Heimbürger et al., 2013; Marty and Chiavérini, 2010; Pasqueron de Fommervault et al., 2015). Such events were responsible of an increase of winter-spring chlorophyll *a* concentration attributed to microphytoplankton (Heimbürger et al., 2013; Marty and Chiavérini, 2010). Therefore, as other urbanized coastal regions, NW Mediterranean Sea is also under the influence of terrestrial inputs and pollution from coastal rivers and small streams (Nicolau et al., 2006) which might deeply impact phytoplankton communities and participate to the current unpredictability of its dynamic.

Here, we investigate decadal microphytoplankton community variations in the highly urbanized semi-enclosed Toulon Bay located in Ligurian Basin impacted by both offshore (wintering deep mixing vents) and terrestrial (anthropogenic) influences to extract main shifts at interannual scale. Main objectives were i) to investigate main microphytoplankton community shifts at a decadal scale within the 2005–2017 period, ii) to describe changes in communities at the taxonomical level using cell biovolumes, iii) to correlate this changes to meteorological modulations or water descriptors, iv) to compare microphytoplankton variations with main phytoplankton biomass proxy (chlorophyll *a* concentration) and v) to propose mechanisms of changes focusing on trophic preferences.

2. Materials and methods

2.1. Study site

Toulon Bay is a Mediterranean semi-enclosed coastal zone near the Toulon agglomeration (~428 000 inhabitants) which extends over 367 km^2 at the south-east of France (43°05′ N – 05°55' E). The bay is divided by an artificial breakwater facing north/south into two connected basins. The West part called "Little Bay" is characterized by smaller and narrower dimensions and is particularly submitted to human influences such as harbour activities (commercial, military and shipyard) or urban runoff mainly driven by the Las river (Pougnet et al., 2014; Tessier et al., 2011). The larger and deeper eastern part named "Large Bay" (42 km^2 and ~17 m deep) is directly open to the Mediterranean Sea (Fig. 1), benefiting from the influence of the Northern Current (Taupier-Letage et al., 2013) which generates a general weak cyclonic circulation into the bay whose intensity is correlated to wind regime (Dufresne et al., 2014; Tessier et al., 2011). Therefore, as other coastal region of Ligurian Basin, Large Bay also host coastal current instabilities like "eddies" which are involved in setting up of punctual coastal spring blooms (Casella et al., 2014). Large Bay is also impacted by diverse terrestrial input sources whose main is the flooded Eygoutier River. As a typical Mediterranean river, the Eygoutier flow shows seasonal fluctuations (from 10 $m^3 h^{-1}$ to 40.10^3 $m^3 h^{-1}$ during dry winter and summer and wet spring and fall, respectively) in connection to the local precipitation rate (Nicolau et al., 2012, 2006). Both the hydrographic regime and the large Eygoutier watershed (~70 km^2) covering urban, rural and industrial zones, have led to high organic matter discharges (2300 $t.an^{-1}$), nitrate enrichment and metallic contamination (Cu, Pb and Zn) during high runoff periods (Nicolau et al., 2006). To a less extent, presence of outfall pipe from AmphorA waste-

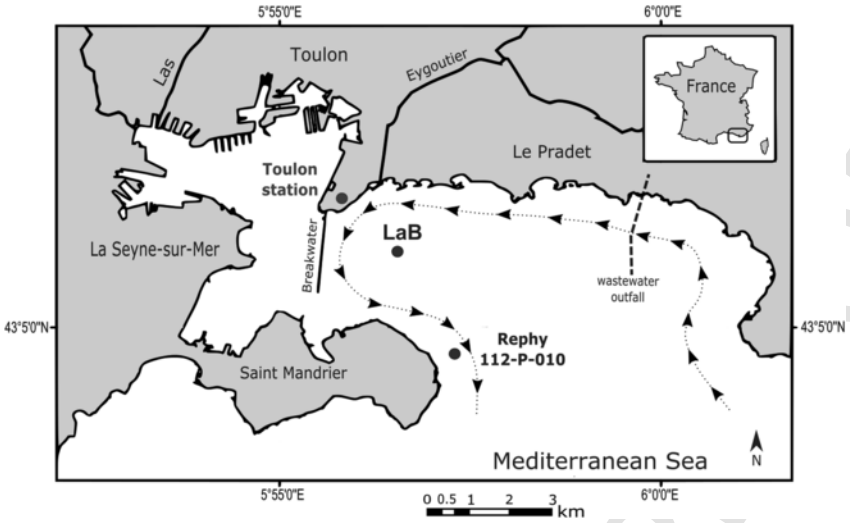

Fig. 1. Map of Toulon Bay with location of the Large Bay phytoplankton sampling site (LaB) and the REPHY sampling site (Rephy 112-P-010). The meteorological Toulon station was also identified (black points), as well as The Eygoutier River and AmphorA wastewater outfall flowing to the Large Bay. Main cyclonic circulation of the Large bay was also specified (adapted from Dufresne et al. (2014)) (dotted arrowed line).

water plant could represent another source of organic matter (~90 t. an^{-1}).

2.2. Plankton sampling

Monthly monitoring of microphytoplankton was realized on "Large Bay sampling point" (LaB) (43°05′45'' N; 05°56′30'' E), located at 1 km from the Eygoutier outfall, from January 2005 to November 2017 and between 8:00 to 11:00 a.m. For microphytoplankton, 10–20 L were collected at 3 m depth using a Niskin sampling bottle. Samples were concentrated into a final volume of 50 ml using inverse filtration (Dodson and Thomas, 1964), and fixed with a 0.3% lugol solution. Because it was dissolved by fixation method, coccolithophorids were not considered in this study. Finally, counts and identification were performed after a 24 h column sedimentation as recommended by Lund et al. (1958) and Utermöhl (1958) by using a phase-contrast microscopy (Leica DMI 4000; magnitude ×400). As described by the Utermöhl method at least 20 fields and 200 cells were counted by sample and abundances were computed as followed:

$$N_{ij} = \frac{\left(\frac{n_{ij}}{f_j}.F_j\right)}{V_j}$$

With N_{ij} the abundance of the species i in a sample j (cell.l^{-1}), n_{ij} the number of cells of the species i, f_j the number of fields counted in sample j, F_j total number of fields, V_j volume of sample j.

To focus on main community changes, selection of representative taxa was performed. A threshold of 10% was applied to both occurrence throughout the time series and relative abundance in at least one sample. Finally, 57 taxa were selected of which 25 diatoms, 22 dinoflagellates and 10 taxa belonging to micro- and upper size classes from nanoflagellates (microflagellates, hereafter) (Table 1).

2.3. Environmental data

Temperature, salinity and chlorophyll *a* concentration monthly time-series from REPHY sampling point ("Rephy 112-P-010": 43° 04′44''N; 5° 57′17''E) located in the Large Bay (Fig. 1) were extracted from Quadrige[2] database, grouping French metropolitan coastal stations belonging to the "Observation and Monitoring Network for Phytoplankton and Hydrology in Coastal Water" (REPHY). The aim of this network implemented by the "French Research Institute for Exploitation of the Sea" (IFREMER) results in the monitoring of phytoplankton, phytotoxic species and hydrology of french coastal areas and valuation of calibrated dataset (Belin et al., 2017). In accordance to the REPHY protocol, surface temperature and salinity were assessed using *in situ* sensor, chlorophyll *a* concentration was evaluated at 1 m depth using monochromatic spectrophotometry or fluorimetry method (Aminot and Kérouel, 2004). Therefore, environmental dataset was completed with monthly rainfall rate (average in mm) from Météo France meteorological Toulon station (43° 06′11''N; 5° 55′ 52''E).

Nitrite/nitrate and phosphate ($NO_2^- + NO_3^- = N\text{-}NO_x^-$ and $P\text{-}PO_4^{3-}$, hereafter) concentrations were monthly measured at "LaB" between January 2005 and March 2007 and between March and December 2015. Using 10 L sampled at 3 m depth, concentrations were obtained following the method proposed by Murphy and Riley (1962) and Tréguer and Le Corre (1975) modified by Strickland and Parsons (1968) for $N\text{-}NO_x^-$ and $P\text{-}PO_4^{3-}$, respectively. Supplementary $N\text{-}NO_x^-$ and $P\text{-}PO_4^{3-}$concentration data from "112-P-010-22B" sampling station and measured at 3 m depth using flow spectrophotometry between March 2009 and March 2010 were added to previous measures. (For more information, see Aminot and Kérouel (2007)).

2.4. Data analysis

2.4.1. Data partitioning

The identification of main and persistent changes into microphytoplanktonic community and environmental conditions across the 2005–2017 period were evaluated using chronological clustering (Legendre et al., 1985). This partitioning method constrained the gathering of dates with adjacent ones allowing to identify homogeneous period. The chronological clustering was applied on log-Chord and Euclidean matrix distance, for microphytoplankton and environmental datasets respectively. Log-Chord distance (Legendre and Borcard, 2018) was the computation of Chord distance:

$$y''_{ij} = \frac{y'_{ij}}{\sqrt{\sum_{i=1}^{p}\left(y'_{ij}\right)^2}}$$

Table 1
Summary of representative micro-phytoplankton taxa features with average abundance (Ab), respective standard deviation and mean contribution in total phytoplankton abundance (Cont) respectively for P_1, P_2, P_3, and overall the 2005–2017 period (Tot); name abbreviation (Abb); geometric cellular shape associated (Shape); mean cellular biovolum (Biov); corresponding lifeform (Lifeform): diatoms (Diat), micro-flagellates (Fla), small dinoflagellates (s.Dino) and large dinoflagellates (L.Dino); trophic status reported in literature for dinoflagellate with references: H: Heterotrophic M:Mixotrophic. A:Autotrophic. (): trophic status was suggested. ?: absence of trophic preference data.

Class	Species	Abb	Ab	Cont (%)				Shape	Biov	Life form	Trophic status
			($ind.l^{-1}$)	Tot	P_1	P_2	P_3		(μm^3)		
Diatoms	*Pseudonitzschia delicatissima*	P.del	2′791 ± 11′437	11.8	15.5	24.3	17.8	prism on parallelogram base	536	Diat	A
	Chaetoceros spp.	Chae	6′057 ± 47′102	10.4	20.8	15.8	8.4	2 cônes	2′612	Diat	A
	Cyclotella spp.	Cyc	388 ± 1′528	6.8	5.8	10.1	8.2	cylinder	2′521	Diat	A
	Thalassionema spp.	Tnema	409 ± 1′773	4.6	6.7	7.7	3.3	cylinder	1′695	Diat	A
	Leptocylindrus danicus	L.dan	1′270 ± 7′902	3.8	14.8	0.7	12.5	cylinder	2′679	Diat	A
	Guinardia spp.	Gui	192 ± 575	3.7	3.7	11.1	6.4	cylinder	33′384	Diat	A
	Cylindrotheca closterium	C.clo	167 ± 548	2.1	5.3	1.6	5.3	cylinder	426	Diat	A
	Pseudonitzschia seriata	P.ser	437 ± 3′030	1.4	10.3	1.4	2.9	prism on parallelogram base	1′419	Diat	A
	Actinoptychus spp.	Act	23 ± 58	1.2	2.4	3.3	0.0	cône + half sphere	9′531	Diat	A
	Coscinodiscus spp.	Cos	21 ± 37	1.2	0.7	4.5	0.5	elliptic prism	140′122	Diat	A
	Dactyliosolen fragilissimus	D.fra	168 ± 938	1.1	11.1	0.2	0.0	cylinder	21′657	Diat	A
	Nitzschia spp.	Nit	48 ± 172	0.8	0.8	1.9	1.8	prism on parallelogram base	15′161	Diat	A
	Skeletonema costatum	S.cos	628 ± 6′583	0.8	3.2	2.0	0.0	cylindre	1′927	Diat	A
	Licmophora gracilis	L.gra	17 ± 67	0.6	2.2	1.7	0.5	gomphonemoid	2′653	Diat	A
	Navicula spp.	Nav	19 ± 37	0.6	1.5	1.2	0.7	elliptic prism	14′833	Diat	A
	Rhizosolenia spp.	Rhi	33 ± 156	0.6	1.0	2.8	1.0	cylinder	247′143	Diat	A
	Bacteriastrum delicatulum	B.del	141 ± 894	0.5	3.8	0.0	0.0	cylinder	2′867	Diat	A
	Asterionellopsis glacialis	A.gla	192 ± 1883	0.4	2.1	0.0	0.6	cylinder	496	Diat	A
	Pleurosigma spp.	Pleu	9 ± 22	0.4	0.8	1.6	0.3	prism on parallelogram base	20′863	Diat	A
	Thalasiosira spp.	Tsira	29 ± 96	0.3	1.2	0.0	0.6	parallelepiped	10′941	Diat	A
	Gyrosigma spp.	Gyros	3 ± 9	0.2	0.7	0.4	0.0	prism on parallelogram base	19′274	Diat	A
	Lioloma spp.	Lio	1 ± 6	0.2	0.4	2.6	0.1	cylinder	30′598	Diat	A
	Pseudonitzschia sp.	Pseu	9 ± 95	0.2	0.1	2.8	0.0	prism on parallelogram base	5′150	Diat	A
	Fragilariopsis cylindrus	F.cyl	2 ± 16	0.1	1.2	0.0	0.0	prism on elliptic base	2′276	Diat	A
	Hemiaulus hauckii	H.hau	5 ± 22	0.1	0.8	0.0	0.0	cylinder	19′721	Diat	A
	Mean		**13′059**	**53.3**	**61.1**	**57.3**	**39.8**				
Micoflagellates	*Hillea fusiformis*	H.fus	461 ± 1′314	6.1	4.8	6.9	12.2	cône + half sphere	316	Fla	A
	Chlorella sp.	Chlo	314 ± 915	3.3	2.2	8.6	6.8	sphere	503	Fla	A
	Dictyocha spp.	Dict	75 ± 224	2.3	5.9	3.4	3.4	sphere	6′587	Fla	A
	Chromulina sp.	Chro	18 ± 61	0.6	2.9	0.7	0.0	sphere	856	Fla	(M) (15)
	Leucocryptos sp.	Leu	18 ± 59	0.4	2.4	0.3	0.0	cône + half sphere	198	Fla	H (13)
	Rhodomonas sp.	Rho	46 ± 207	0.4	0.3	0.6	1.7	cône + half sphere	1′059	Fla	A
	Hemiselmis sp.	Hemi	23 ± 97	0.3	0.1	0.1	2.4	prolate spheroid	983	Fla	M (15)
	Chlamydomonas sp.	Chla	6 ± 22	0.2	1.6	0.0	0.2	sphere	1′544	Fla	M (19)
	Heterosigma sp.	Het	10 ± 52	0.2	0.9	0.5	0.3	cône + half sphere	1′425	Fla	A
	Tetraselmis spp.	Tet	55 ± 363	0.2	0.3	0.0	1.6	prolate spheroid	1′488	Fla	(M) (5)
	Mean		**1′026**	**14.2**	**12.8**	**11.7**	**34.0**				
Dinoflagellates	*Gymnodinium* spp.	Gym.spp	760 ± 1′751	13	16.6	8.6	10.2	ellipsoïd	6′338	s.Dino	M (2,11,18)
	Ceratium furca	C.fur	39 ± 71	2	1.9	6.1	0.5	prolate spheroid + 2 cones + cylinder	59′072	L.Dino	M (7,8,11,18)
	Prorocentrum micans	P.mic	48 ± 130	1.8	1.4	5.5	1.8	prolate spheroid	9′634	s.Dino	M (11,17,18)
	Prorocentrum arcuatum	P.arc	32 ± 76	1.7	1.2	5.7	0.3	prolate spheroid	23′125	L.Dino	?
	Scrippsiella spp.	Scri	61 ± 166	1.5	2.8	2.8	0.3	prolate spheroid	7′701	s.Dino	M (11,21)
	Achradina spp.	Achr	43 ± 121	1.1	2.9	1.7	0.9	prolate spheroid	3′116	s.Dino	(H) (16)
	Alexandrium spp.	Alex	22 ± 54	0.7	1.7	2.7	0.5	prolate spheroid	7′968	s.Dino	M (3,11)
	Ceratium fusus	C.fus	11 ± 19	0.5	0.6	1.5	0.1	2 cônes	10′679	s.Dino	M (11. 18)
	Oxytoxum spp.	Oxy	27 ± 164	0.5	0.7	0.9	1.6	prolate spheroid	6′065	s.Dino	H (7)
	Gyrodinium sp.	Gyrod	48 ± 229	0.4	0.2	0.8	1.6	ellipsoïd	13′480	s.Dino	M (11,18)
	Goniodoma sp.	Gon	7 ± 18	0.3	0.5	1.3	0.1	sphere	63′809	L.Dino	?
	Gonyaulax spp.	Gony	7 ± 14	0.3	0.6	0.6	0.1	cône + half sphere	37′431	L.Dino	M (3,6)
	Protoperidinium divergens	P.div	8 ± 19	0.3	0.1	1.3	0.2	2 cônes	46′645	L.Dino	H (10,11)
	Protoperidinium pellucidum	P.pel	5 ± 15	0.3	0.4	1.4	0.1	2 cônes	23′324	L.Dino	H (11)

Table 1 (*Continued*)

Class	Species	Abb	Ab	Cont (%)				Shape	Biov	Life form	Trophic status
			(ind.l^{-1})	Tot	P_1	P_2	P_3		(μm^3)		
	Protoperidinium pentagonum	P.pen	5 ± 18	0.3	0.4	1.3	0.0	2 cônes	156′799	L.Dino	H (11)
	large *Protoperidinium* spp.	Prot.L	6 ± 19	0.3	0.0	1.6	0.1	prolate spheroid	17′548	L.Dino	H (11)
	Amphidinium spp.	Amp	12 ± 76	0.2	1.3	0.1	0.5	ellipsoïd	1′838	s.Dino	(M) (11,21)
	Amylax spp.	Amy	4 ± 12	0.2	0.3	0.9	2.0	cône + half sphere	5′054	s.Dino	(M) (9,14)
	Ceratium penatogonum	C.pen	3 ± 8	0.2	0.3	1.3	0.1	prolate spheroid + 2 cones + cylinder	101′915	L.Dino	?
	Corythodinium sp.	Cor	6 ± 21	0.2	0.9	0.6	0.0	2 cônes	4′026	s.Dino	?
	Dinophysis acuminata	D.acu	5 ± 13	0.2	0.2	0.8	0.4	ellipsoïd	22′266	L.Dino	M (1,9,12)
	small *Protoperidinium* spp	Prot.s	9 ± 38	0.2	0.9	0.0	0.2	2 cônes	7′043	s.Dino	H (11)
	Mean		**1′168**	**26.0**	**26.1**	**31.0**	**26.2**				

Notes: (1) Berland et al. (1995); (2) Bockstahler and Coats (1993); (3) Brahim et al. (2015); (4) Buric et al. (2009); (5) Cid et al. (1992); (6) Hansen et al. (1996); (7) Ignatiades (2012); (8) Ignatiades and Gotsis-Skretas (2010); (9) Jacobson and Anderson (1996); (10) Jeong (1994); (11) Jeong et al. (2010); (12) Kim et al. (2008); (13) Novarino et al. (1997); (14) Park et al. (2013); (15) Saad et al. (2016); (16) Sakka et al. (2000); (17) Shim et al. (2011); (18) Stoecker (1999); (19) Weithoff and Wacker (2007); (20) Yamaguchi and Horiguchi (2005) (21) Yoo et al. (2010);

On log-transformed data count:

$$y'_{ij} = \log_e\left(y_{ij} + 1\right)$$

Where y_{ij} was the abundance of species *i* in sampling *j*.

As determined by the authors, log-chord distance was particularly useful to normalize highly asymmetrical count data while retaining chord distance properties (*e.g.* low weight for rare species and low counts) (Legendre and Gallagher, 2001).

Influence of partitioning as well as months, years and interannual variability (Months x Years) on microphytoplankton assemblage was evaluated using non-parametric PERmatutional Multivariate ANalysis Of Variance (PERMANOVA) analysis performed on distance matrix (Anderson, 2001).

Considering the scarcity of nutrient data, only water temperature, salinity and rainfall rate were used to describe environmental conditions in clustering analysis using the euclidean distance.

2.4.2. Univariate shift detection method

Mean shift detection in univariate variables were performed using "Binary Segmentation" algorithm (from r package "changepoint") which was a sequential method minimizing the sum of costs and allowing to detect optimal segmentation (for more informations see Killick and Eckley (2014)). To avoid seasonal detection and to focus on long-term changes, a maximum of 3 main change points with a minimum segment length of 24 months were considered. Significance of extracted periods was evaluated using post-hoc non-parametric Krukall-Wallis pairwise comparison with Bonferroni correction (PMCMR r Package). Furthermore, loess regression (α = 0.3) was computed on 12-month moving average to summarize the interannual trend of each variable.

2.4.3. Assemblage characterization and community changes

The communities relating to different periods previously extracted were identified using the "Group-equalized Indicator Value index" (IndVal ^{g}) (De Cáceres et al., 2010; De Cáceres and Legendre, 2009) which was the improved version of IndVal index (Dufrene and Legendre, 1997) adapted for unbalanced size groups.

$IndVal^g_{ij}$ summarized *i* species affinity for *j* period by computing its "Specificity" $\left(A^g_{ij}\right)$ and "Fidelity" (B_{ij}) component:

$$IndVal^g_{ij} = A^g_{ij} * B_{ij} * 100$$

"Specificity" may be traduced as the relative abundance of species during a specific period and was computing as follow:

$$A^g_{ij} = \frac{N_{ij}/Nsamp_j}{\sum_{j=1}^{J} Nij/Nsampj}$$

With N_{ij} the sum of abundance of species i during period j, $Nsamp_j$ the number of samples belonging to period *j* and *J* the total number of period *j*.

While "Fidelity" quantifies the frequency with which a species was found in the target period compared to the whole time series:

$$B_{ij} = \frac{O_{ij}}{Nsamp_j}$$

With O_{ij} number of occurrence of species *i* within the target period *j*.

Then significance of each IndVal^g was evaluated computing 10′000 random permutations of samples by bootstrapping. For each species, IndVal^g with single period association was first computed in order to identify indicator species. Then, the same association measure but involving combination of periods was performed to identity communities associated with more than one period.

For each season, the relative influence of phytoplankton groups (diatoms, dinoflagellates and microflagellates) on time-serie partitioning were also evaluated using ANOSIM (see appendix A).

As mixotrophy is a widespread strategy among dinoflagellates (Stoecker, 1999), trophic status (*i.e.* autotrophic, mixotrophic or heterotrophic) were identified for dinoflagellate and also for microflagellate taxa from the literature reports to focus the interpretation of community changes on trophic preferences (Table 1).

2.4.4. Size variations

To investigate variations in size structure, species-specific cell biovolumes (μm^3) were computed from geometric shapes described in Hillebrand et al. (1999), Sun and Liu (2003) and Vadrucci et al. (2007, 2013) using cell linear dimensions collected by inverted microscopy between 2005 and 2013. Missing dimensions were extrapolated using allometric ratios computed from Olenina et al. (2006) database (see appendix B, for details).

To evaluate size variations in communities, mean cell biovolumes were computed for the three main microphytoplankton classes (i.e. di-

atoms, dinoflagellates and microflagellates) as followed:

$$mBv = \frac{\sum_i^p (N_i * Bv_i)}{Ntot}$$

With *Ntot* the total abundance of the specific class, *N* and *Bv* abundance and biovolume of *i* taxa, respectively.

Comparisons between periods were performed using a non-parametric pairwise Wilcoxon rank test with Bonferonni correction. In the case of significant changes in mean biovolumes between periods, different "lifeforms" were investigated in diatoms and dinoflagellates to detect changes in life-strategies in these two classes. Here, lifeforms were defined as biovolume classes characterizing change in community abundance between two consecutives periods. A linear regression model was used to identify mean biovolumes for which we observed a shift in abundance between periods (see appendix C, for details). Due to biases caused by the sampling methodology used, microflagellate community was considered as a unique lifeform. To compare interannual dynamics from lifeforms, Spearman correlation was then performed on yearly average values of standardized abundance anomalies (deviation from monthly mean abundance divided by standard deviation) for each season.

3. Results

3.1. Time partitioning

The concomitance of 2 major interannual changes was identified between "environmental" and "microphytoplankton community" datasets using chronological clustering, leading to the distinction of 3 periods (P_1, P_2 and P_3) (Fig. 2). First change was observed during late-fall 2008 and spring 2009 and a second during winter 2015 and at the end of 2015, in environmental and microphytoplankton datasets respectively (see appendix D). Despite the uncertainty about the timing of the second change point in microphytoplankton composition due to a lack of data during 2015, PERMANOVA analysis indicated the significance of the partitioning (pval < 0.01) (Table 2). However, the partitioning explained less the total variance rather than annual or interannual variability (R^2 = 6, 13 and 17% respectively for "Period", "Months" and "Years" factors, respectively).

3.2. Environmental variability and nutrients

Analysis of univariate environmental data showed that period partitioning was primarily driven by changes in the rainfall rate (Fig. 3a). P_1 was characterized by a relative low precipitation rate (~27 ± 48 mm), associated with a high and stable salinity in the Large Bay (~38.1 ± 0.5). Conversely, P_2 showed an increase of rainfall (~68.8 ± 59.9 mm), particularly during winter 2008/2009 which led to a brutal and persistent decrease of salinity in the Large Bay (~35.6 ± 1.2) detected from the end of 2008 until early 2011. Despite the maintenance of a high rainfall rate over the period 2009–2015, the increase in salinity trend was observed in 2011 and has conserved a relative steady state until the end of 2017 (~37.4 ± 1.19) (Fig. 3b). Finally, from early 2015 rainfall rate showed a significant and sudden reduction until the end of 2017 (~28.9 ± 28.6 mm). Seasonal variations in rainfall rate described a classical Mediterranean precipitation pattern with lowest values during summer and higher during late-fall/early-winter season (mean of 4.5 and 88.1 mm, respectively). The latest season was particularly impacted by the intensification of rainfall rate during P_2 (mean of 114 ± 15 mm between October to January) (Fig. 3d). Similarly, highest differences in salinity between periods were found during the cold season (from November to February, mean of 38.1, 35.8 and 37.5 for P_1, P_2 and P_3, respectively) (Fig. 3e).

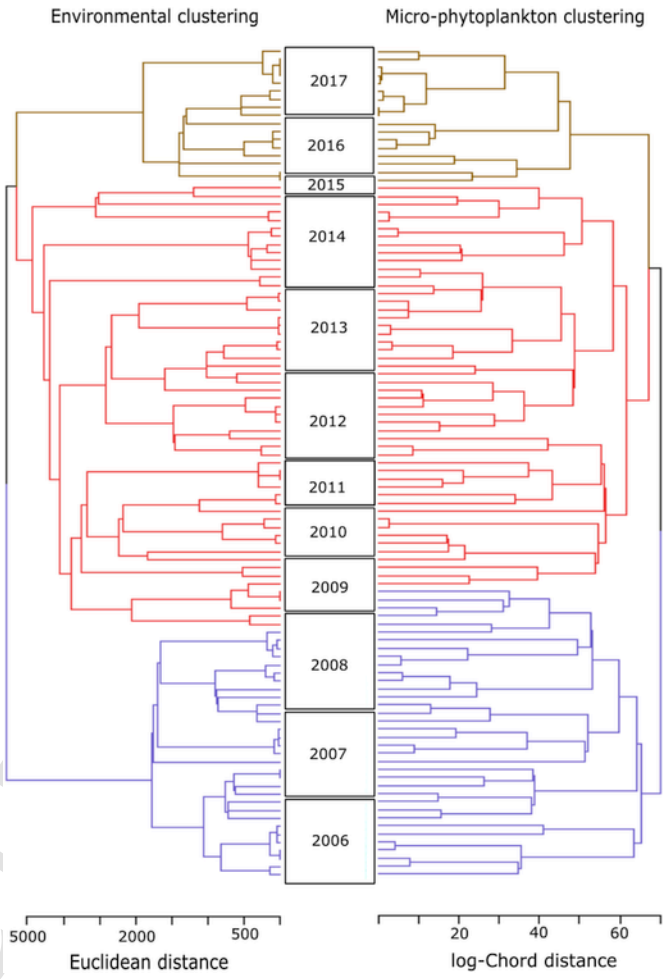

Fig. 2. Comparison of the chronological clusterings performed on the 2006–2017 "environmental" dataset (water temperature, salinity and rainfall rate) using euclidean distance (left cluster) and on the 2005–2017 "micro-phytoplankton community" dataset using log-Chord distance (right cluster). For each dataset, colored branches identified 3 homogeneous periods (P_1, P_2, and P_3 in blue, red and brown) extracted from the 2 main change points (Cut-off levels at h = [3658; 3429] and h = [67.2; 64.4] for the "environmental" and the "micro-phytoplankton" time series, respectively). Asymmetry between year boxes was relative to missing values in biological time-series. (For interpretation of the references to color in this figure legend, the reader is referred to the Web version of this article.)

Table 2
Summary of PERMANOVA analysis testing the influence of the partitioning (Periods), months (Months), years (Years), and their interaction (Months x Years) on log-chord distance of micro-phytoplankton abundance dataset. Df: degree of Freedom. SS: Sum of Squares. F.Model: F statistic from the permutation procedure.

	Df	SS	F.Model	R^2	P-value
Periods	2	4.40	13.4	0.06	***
Months	11	9.20	2.55	0.13	***
Years	12	12.09	3.07	0.17	***
Months x Years	94	40.33	1.31	0.56	***
Residuals				0.09	

***p < 0.001.

Based on incomplete time-series, no significant change were found between 2005 and 2006 (P1) and 2009 early 2010 (P2), nor between 2009 and 2010 (P2) and 2015 (P_3) in $N\text{-}NO_x^-$ (mean of 2.4 ± 4.5; 0.54 ± 0.69 and 1.25 ± 0.88 µmol l^{-1}, respectively) and $P\text{-}PO_4^{3-}$ (mean of 0.09 ± 0.03; 0.03 ± 0.02 and 0.05 ± 0.04 µmol l^{-1}, respectively) concentrations (Fig. 4a and b). $P\text{-}PO_4^{3-}$ annual mean variations showed values ranged between 0.15 µmol l^{-1} in January and 0.03 µmol l^{-1} in

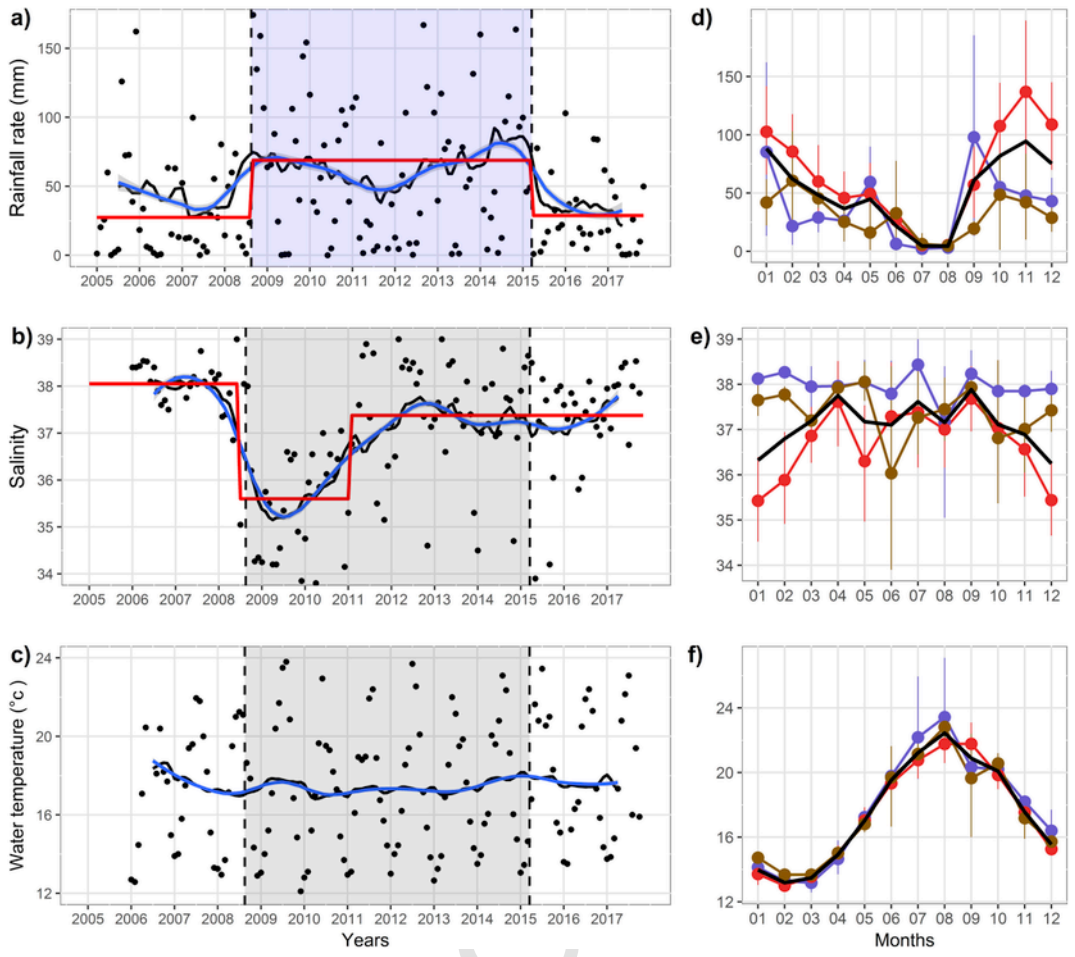

Fig. 3. 2005–2017 time series of rainfall rate (a), salinity (b), and water temperature (c). Moving average (solid black line) and loess filter regression (α = 0.3) (blue line) were performed on raw data (black dots) to summarize the trend. Significant mean changes were indicated by red segments. Shaded area indicated (P_2) wet period delimited by change points (vertical dotted lines) from environmental clustering. Respective mean annual variations (d, e and f) over the 2005–2017 (dark thick line) and the monthly averaged value with non-parametric 0.95 confident interval during each extracted period (blue, red and brown for P_1, P_2 and P_3, respectively). (For interpretation of the references to color in this figure legend, the reader is referred to the Web version of this article.)

June and July with no clear phenological signal (Fig. 4 d). Conversely, $N\text{-}NO_x^-$ concentrations showed a noticeable annual pattern with minima found during late spring/summer (mean of 0.26 µmoll^{-1} between May and August) and higher concentrations found in September (mean of 4.8 ± 9.2 µmoll^{-1}) and winter (mean of 3.3 ± 1.8 µmoll^{-1} between January and March) (Fig. 4c). These two latter peaks were present in (P_1) 2005–2006 (3.1 ± 3.2 and 6.6 ± 11.2 µmol.l-1, respectively) and in (P_3) 2015 data (2.3 and 2 µmoll^{-1}, respectively) but absent during (P_2) 2009–2010 (0.5 ± 0.4 and 0.2 µmoll^{-1}, respectively). Furthermore, P_2 seasonal mean variation exhibited lower concentration values for both nutrients. Finally, water temperature didn't show significant change ($p > 0.05$) in the mean (~17.5 °C) despite a strong seasonal variability with maximum values occurring in August (21.7 ± 1.7 °C) and minimum in February (13.2 ± 0.4 °C) in the 3 periods (Fig. 3c and f).

3.3. General phytoplankton composition

3.3.1. Total microphytoplankton abundance

Total microphytoplankton abundance showed a high range of values from 168 to $7.6.10^5$ cells.l^{-1}, during December 2010 and August 2006, respectively with an average of $1.3.10^4$ cells.l^{-1} (Fig. 5a). The "Binary segmentation" method identified two significant change points identifying 2005–2006, 2007–2014 and 2015–2017 subperiods. The first change occurred during early spring 2007 while the second appeared in early winter 2015 and coincided with the second change in partitioning analysis (Fig. 2). The 2005–2006 subperiod was characterized by a higher average abundance (6.10^4 cells.l^{-1}) and contrasted with lowest average abundance observed during 2007–2014 period (3.10^3 cells.l^{-1}). Finally, second change point was characterized by an increase of total abundance during the 2015–2017 subperiod (mean of 2.10^4 cells.l^{-1}). The latter did not show any significant difference with the 2005–2007 subperiod (pval > 0.05). Clear seasonal pattern was observed over the 2005–2017 period characterized by 2 seasonal blooms occurring in March (4.10^4 cells.l^{-1}) and September (8.10^4 cells.l^{-1}) and with lowest values found in December (2.10^3 cells.l-1) and August (3.10^3 cells.l-1) (Fig. 5c). Global lower average values were observed during P_2, except in October showing higher values than average (mean of $7.8.10^3$ cells.l^{-1}). March abundance peak was identified during each period with high confident interval describing an inter-annual variability of bloom events. Nonetheless the highest bloom values were found during P_1 (7.10^4 in [1.10^3; $1.7.10^5$] cells.l^{-1}) and weakest during P_2 ($1.4.10^4$ in [1.10^3; 4.10^4] cells.l^{-1}). Similarly, late-summer peak was only found during P_1 (2.10^5 in [3.10^3; $5.7.10^5$] cell.l^{-1}) and was missing during P_2 and P_3 (2.8 in [1.10^3; 4.10^3] and $2.6.10^3$ in [1.10^3; 4.10^3] cells.l^{-1}, respectively).

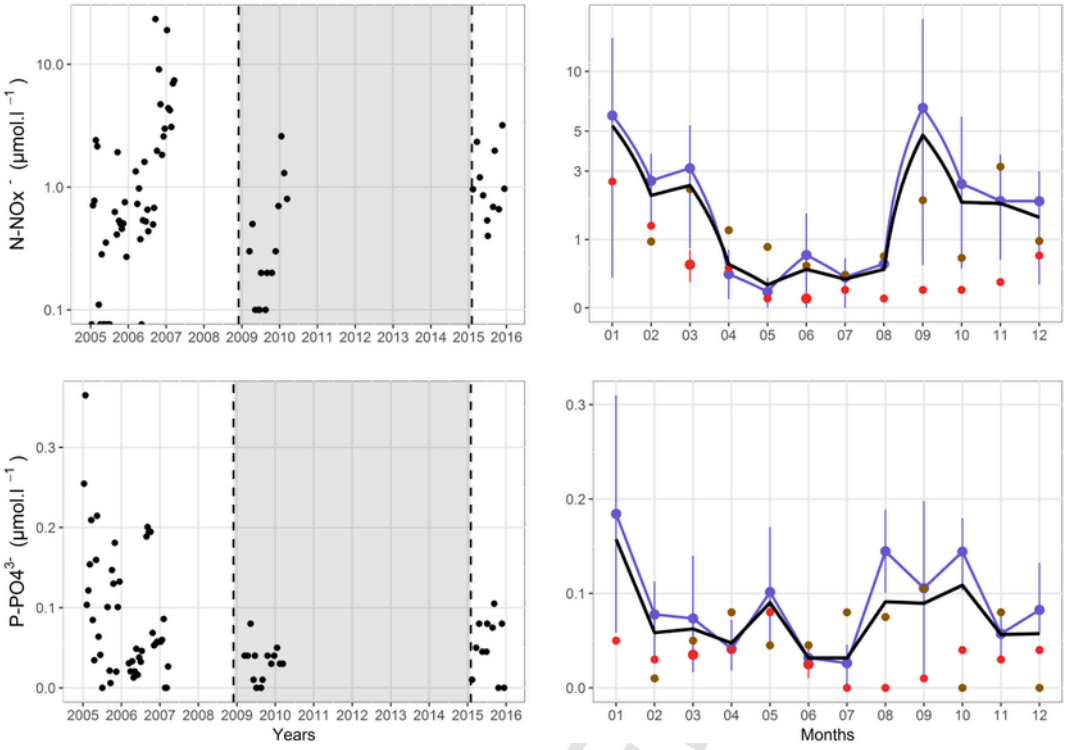

Fig. 4. 2005–2017 N-NO_x^- and P-PO_4^{3-} time series (a and b, respectively) and annual variations (c and d, respectively) over the 2005–2017 period and mean monthly values from P_1, P_2 and P_3 (blue, red and brown, respectively) with non-parametric 0.95 confident interval. Shaded area indicated (P_2) wet period delimited by change points (vertical dotted lines) from environmental clustering. (For interpretation of the references to color in this figure legend, the reader is referred to the Web version of this article.)

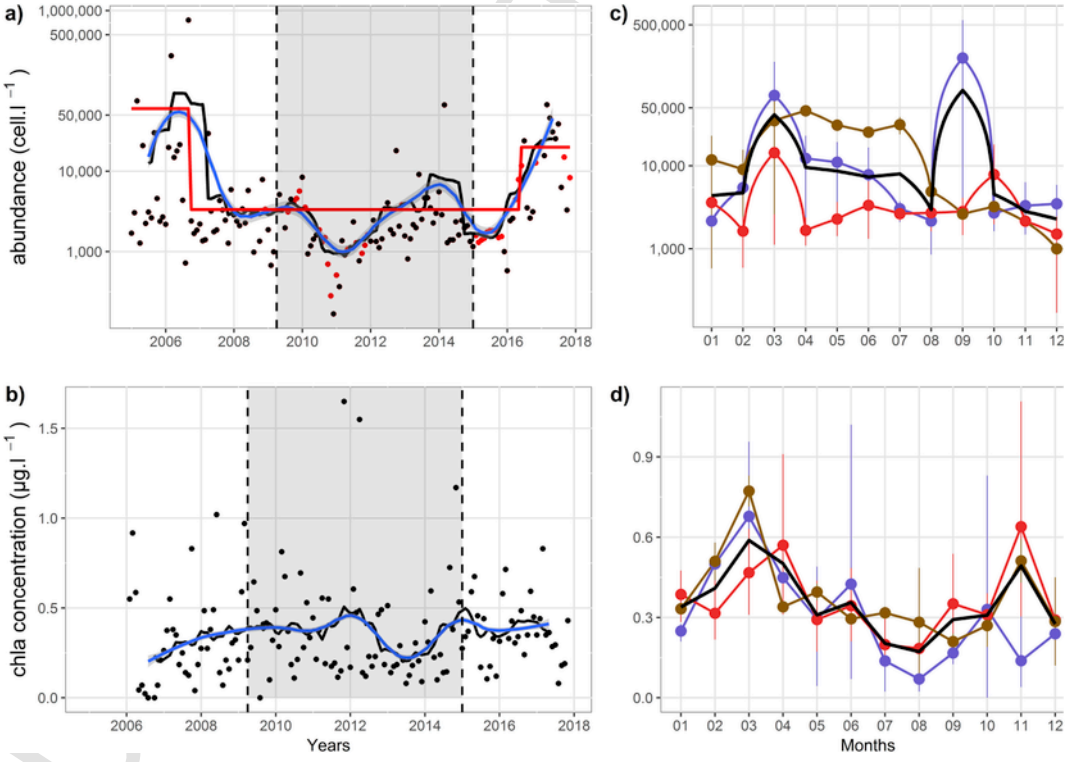

Figure 5. 2005–2017 monthly time series of the total micro-phytoplankton abundance (a) with original (black dots) and interpolated data (red points) and chlorophyll *a* concentration (b). Moving average (solid black line) and loess filter regression (α = 0.3) (blue line) were performed on data to summarize the trend. The red segment indicated significant change in the mean. Vertical dashed line identified change points from biological partitioning and shaded area correspond to (P_2) wet period. Dark thick lines were for monthly averaged variations of total micro-phytoplankton abundance (c) and chlorophyll *a* concentration (d) over the 2005–2017 period. Color lines described monthly averaged values with non-parametric 0.95 confident interval associated at each extracted period (blue. red and brown for P_1. P_2 and P_3, respectively). Total abundance was expressed in log10 scale.

3.3.2. Chlorophyll a concentration

Chlorophyll *a* concentration described a phenological pattern with 2 annual concentration peaks during March–April (mean of $0.59 \pm 0.26\,\mu g.\ l^{-1}$) and in November (mean of $0.49 \pm 0.46\,\mu g\,l^{-1}$) (Fig. 5d). Globally, all periods showed spring blooms with higher values found in March during P_3 and P_1 (mean of 0.77 ± 0.08 and $0.68 \pm 0.33\,\mu g\,l^{-1}$, respectively) and in April during P_2 (mean of $0.47 \pm 0.22\,\mu g\,l^{-1}$). Otherwise, the November peak was only identified during P_2 and P_3 (0.64 ± 0.56 and $0.51 \pm 0.11\,\mu g\,l^{-1}$). No significant difference was observed between periods (pval > 0.05).

Despite the absence of significant change in mean values, loess regression on moving average trend showed a gradual increase of the phytoplankton biomass in early 2008 (from 0.28 ± 0.26 to $0.41 \pm 0.33\,\mu g\,l^{-1}$) (Fig. 5b). The most important change in trend observed was a decrease of the chlorophyll *a* concentration from spring 2012 to fall 2014 (from 0.41 ± 0.22 to $0.25 \pm 0.14\,\mu g\,l^{-1}$). Finally, both loess regressions ($\alpha = 0.3$) on total abundance and on chlorophyll *a* concentration showed significant negative spearman correlation (rho = −0.61, pval < 0.01).

3.3.3. Microphytoplankton composition

Diatoms were dominant in total microphytoplankton abundance, during the whole 2005–2017 period (53.3% on average) as well as in the three extracted periods (61.1%, 57.3% and 39.8%, for P_1, P_2 and P_3, respectively) mostly due to the main representative taxa: *P. delicatissima*, *Chaetoceros* spp., *Cyclotella* spp., *Thalassionema* spp. and *L.danicus* (Table 1). Dinoflagellate group was the second most represented, especially during P_2 (~31%), driving by abundant species (*e.g. C. furca*, *P. micans*, *P.arcuatum*, *Alexandrium* spp.). However, the most abundant dinoflagellate taxa *Gymnodinium* spp. showed the highest mean contribution during P_3 (10.2%). Globally microflagellates were less abundant over the 2005–2017 period (14.2%) but were identified as the second contributor in total abundance during P_3 (34%) driven by abundant autotrophic species *H. fusiformis* and *Chlorella* sp. (12.2 and 6.8%, respectively).

3.4. Changes in microphytoplankton assemblage

Among the 57 selected taxa, 21, 13 and 23 were respectively associated to P_1, P_2 and P_3 from the single $IndVal^g$ index (Table 3). P_1 community was mostly composed of diatoms (13 out of 26 diatom taxa selected) and mixo/heterotrophic microflagellates (8 out of 15) (Table 1). Among the most abundant taxa, it was possible to mention *Chaetoceros* spp. (0.83), *L. danicus* (0.76), *D. fragilissimus* (0.60), *B. delicatulum* (0.50), *H. hauckii* (0.49) for diatoms and *Leucocryptos* sp. (0.59), *Chlamydomonas* sp. (0.44), *Chromulina* sp. (0.40) for microflagellates. Some dinoflagellates species as *Scripssiella* sp., *Achradina* sp., *Corythodinium* sp. and small *Protoperidinium* spp. also exhibited high but not significant association values (0.56; 0.42; 0.33 and 0.31, respectively). Combined $IndVal^g$ index, which allowed an association of 2 periods, showed that some of P_1 indicator taxa such as *Chaetoceros* spp., *Chlamydomonas* sp., *Thalasionema* spp. displayed higher association values for P_1 and P_3 combination (0.86; 0.45 and 0.85, respectively).

Conversely, 10 of the 23 dinoflagellate taxa were significantly associated to P_2 and particularly *P. arcuatum* (0.80), *C. furca* (0.72), *C. fusus* (0.57), *P. divergens* (0.48), *Gonyaulax* sp. (0.43), large *Protoperidinium* spp. (0.40) and *P. pentagonum* (0.39). Some diatom taxa such *Actinoptychus* sp. and in a less extent *Coscinodiscus* spp. were also associated with P_2 (0.73 and 0.48, respectively). Among these P_2 indicators, some dinoflagellates such as *C. fusus*, *P. divergens*, *Gonyaulax* sp. or *D. acuminata* were more associated with the "P_2 & P_3" combination. Only the dinoflagellate species *C.furca* (0.77) and the diatom taxa *Coscinodiscus* spp. (0.60) showed association with P_1 and P_2. In addition, ANOSIM

Table 3
Summary of single and combined association measure ($IndVal^g$) of representative microphytoplankton taxa with statistical significance of indexes: * <0.05; ** <0.01; *** <0.001.

		Single		Combined	
Taxa	Class	Period	$IndVal^g$	Period	$IndVal^g$
Chaetoceros spp.	Diatom	1	0.834*	1 + 3	0.868*
Leptocylindrus danicus	Diatom	1	0.756***	1	0.756**
Dactyliosolen fragilissimus	Diatom	1	0.600**	1	0.600**
Leucocryptos sp.	Flagellate	1	0.593**	1	0.593**
Bacteriastrum delicatulum	Diatom	1	0.500**	1	0.500**
Hemiaulus hauckii	Diatom	1	0.486**	1	0.486**
Chlamydomonas sp.	Flagellate	1	0.444*	1 + 3	0.45*
Chromulina sp.	Flagellate	1	0.397*	1	0.397*
Thalassionema spp.	Diatom	1	0.728	1 + 3	0.848 *
Scrippsiella spp.	Dinoflagellate	1	0.559	1 + 3	0.69
Pseudonitzschia delicatissima	Diatom	1	0.552	1 + 2	0.694
Achradina spp.	Dinoflagellate	1	0.423	1 + 3	0.594
Asterionellopsis glacialis	Diatom	1	0.413	1	0.413
Pseudonitzschia seriata	Diatom	1	0.392	1 + 3	0.448
Skeletonema costatum	Diatom	1	0.39	1	0.39
Gyrosigma sp.	Diatom	1	0.35	1 + 2	0.402
Corythodinium sp.	Dinoflagellate	1	0.328	1 + 3	0.382
Heterosigma sp.	Flagellate	1	0.323	1 + 3	0.367
small *Protoperidinium* spp.	Dinoflagellate	1	0.312	1 + 3	0.486
Fragilariopsis cylindrus	Diatom	1	0.167	1	0.167
Lioloma sp.	Diatom	1	0.143	1 + 2	0.156
Prorocentrum arcuatum	Dinoflagellate	2	0.795***	2	0.795***
Actinoptychus spp.	Diatom	2	0.726***	2	0.726***
Ceratium furca	Dinoflagellate	2	0.722***	1 + 2	0.766 **
Ceratium fusus	Dinoflagellate	2	0.565*	2 + 3	0.587*
Protoperidinium divergens	Dinoflagellate	2	0.483*	2 + 3	0.544*
large *Protoperidinium* spp.	Dinoflagellate	2	0.398*	2 + 3	0.489 **
Protoperidinium pentagonum	Dinoflagellate	2	0.388*	2	0.388*
Coscinodiscus spp.	Diatom	2	0.486	1 + 2	0.608
Dinophysis acuminata	Dinoflagellate	2	0.374	2 + 3	0.467 *
Amylax spp.	Dinoflagellate	2	0.325	2 + 3	0.371
Ceratium penatogonum	Dinoflagellate	2	0.32	1 + 2	0.354
Gonyaulax spp.	Dinoflagellate	2	0.282	2 + 3	0.466
Pseudonitzschia sp.	Diatom	2	0.194	2	0.194
Rhodomonas sp.	Flagellate	3	0.932***	3	0.932***
Hillea fusiformis	Flagellate	3	0.930***	3	0.930***
Chlorella sp.	Flagellate	3	0.922***	3	0.922***
Gymnodinium spp.	Dinoflagellate	3	0.895***	1 + 3	0.969 ***
Cyclotella spp.	Diatom	3	0.884**	2 + 3	0.923 ***
Nitzschia spp.	Diatom	3	0.839***	3	0.839***
Gyrodinium sp.	Dinoflagellate	3	0.830***	3	0.830***
Navicula spp.	Diatom	3	0.784***	3	0.784***
Guinardia spp.	Diatom	3	0.749**	3	0.749**
Prorocentrum micans	Dinoflagellate	3	0.743**	2 + 3	0.754 **
Hemiselmis sp.	Flagellate	3	0.720***	3	0.720***
Oxytoxum spp.	Dinoflagellate	3	0.688**	2 + 3	0.711 **
Amphidinium spp.	Dinoflagellate	3	0.606**	3	0.606**
Alexandrium spp.	Dinoflagellate	3	0.593**	3	0.593**

Table 3 (*Continued*)

		Single		Combined	
Taxa	Class	Period	IndVal[g]	Period	IndVal[g]
Licmophora gracilis	Diatom	3	0.575**	3	0.575**
Tetraselmis spp.	Flagellate	3	0.533*	1 + 3	0.54 *
Pleurosigma sp.	Diatom	3	0.526**	3	0.526**
Thalasiosira spp.	Diatom	3	0.522**	1 + 3	0.540 *
Cylindrotheca closterium	Diatom	3	0.618	1 + 3	0.799 ***
Dictyocha spp.	Flagellate	3	0.575	1 + 3	0.758 **
Rhizosolenia spp.	Diatom	3	0.467	1 + 3	0.511
Goniodoma sp.	Dinoflagellate	3	0.393	2 + 3	0.490 **
Protoperidinium pellucidum	Dinoflagellate	3	0.32	2 + 3	0.430 **

analysis identified dinoflagellates as the most impacted group by community changes particularly in spring and summer (see appendix A, for details).

Finally, P_3 was mainly associated with autotrophic microflagellates species (*e.g. Rhodomonas* sp. (0.93), *Hillea fusiformis* (0.93), *Chlorella* sp. (0.92) but also with diatom taxa (*e.g. Cyclotella* spp. (0.88), *Nitzschia* spp. (0.84), *Navicula* sp. (0.78), *Guinardia* spp. (0.75)) and some dinoflagellates (*e.g. Gymnodinium* spp. (0.89), *Gyrodinium* sp. (0.83), *P.micans.* (0.74), *Oxytoxum spp.* (0.68)).

3.5. Biovolumes and lifeform variations

Globally, the dinoflagellate community described higher mean cell biovolumes with values ranging from 1.10^4 to 2.10^4 µm^3 (for Q25 and Q75, respectively) during the whole 2005–2017 period (Fig. 6). Diatom mean cell biovolumes were, in turn, ranged between $6.2.10^3$ and $1.3.10^4$ µm^3 (for Q25 and Q75, respectively) and finally, microflagellate community was constituted by lower cell sizes varying between 684 and $2.6.10^3$ µm^3 (for Q25 and Q75, respectively). Contrary to diatom community, dinoflagellates and microflagellates exhibited significant change of mean cell biovolumes between periods (pval < 0.05). Thus, dinoflagellates described an increase of mean cell biovolumes between P_1 and P_2 (from $1.3.10^4$ to $2.2.10^4$ µm^3, respectively) and then a decrease in P_3 (mean of $7.9.10^3$ µm^3), suggesting an important shift within the community. Microflagellates only showed a significant decrease of mean cell biovolume between P_1 and P_2 (from $2.2.10^3$ to $1.7.10^3$ µm^3, respectively), and then conserved low cell sizes during P_3 (mean of $1.1.10^3$ µm^3). As none significant change in mean biovolumes was found for diatoms, the whole diatom community was subsequently considered as a unique lifeform. Conversely, these results led to the consideration of two different lifeforms for dinoflagellates characterizing species with biovolumes lower (small dinoflagellates) and higher (large dinoflagellates) than $1.5.10^3$ µm^3 (see appendix C, for methodological details).

Mean seasonal anomalies of lifeform abundances described different interannual variations over the 2005–2017 period (Fig. 7). First, spring and summer diatom abundances increased mostly during years hosting intense wintering deep mixing in Ligurian Sea (+0.27, +1.59 and in a less extent −0.12 for 2005, 2006 and 2013, respectively) and also in 2017 (+0.63) for which there is no current report in the literature. Spring and summer anomalies of large dinoflagellates were positive during P_2 wet period (mean of +0.57 and + 0.72, respectively) except during spring 2013 (−0.35). In addition, large dinoflagellate variations were negatively correlated to diatoms during spring (rho = -0.91) (see the summary in appendix E). Then, accordingly to seasonal anomalies,

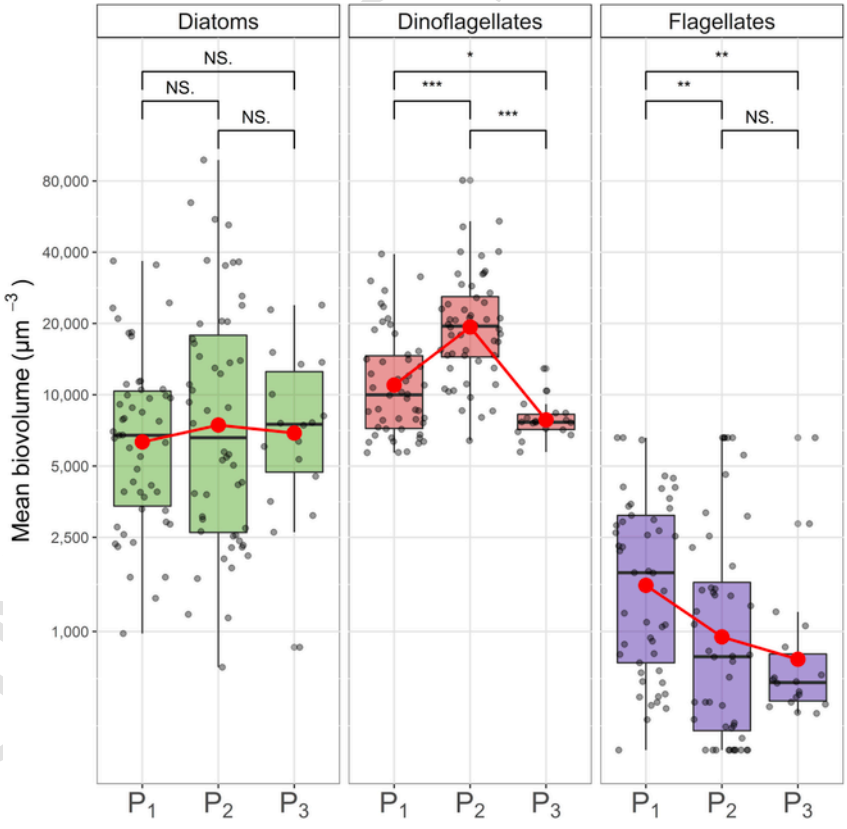

Fig. 6. Mean cell biovolume variations of diatom (left panel), dinoflagellate (middle panel) and micro-flagellate (right panel) communities during the 3 extracted periods (P_1, P_2 and P_3). Black dots were for data, red point indicated averaged values during each period and red line summarized changes in mean. Boxplot indicated values ranged between the 25 and 75th percentile and median values. Results for Wilcoxon pairwise comparison using Bonferroni correction were specified: NS: no significant. * <0.05, ** <0.01, *** <0.001. Values were represented in 10 log scale. (For interpretation of the references to color in this figure legend, the reader is referred to the Web version of this article.)

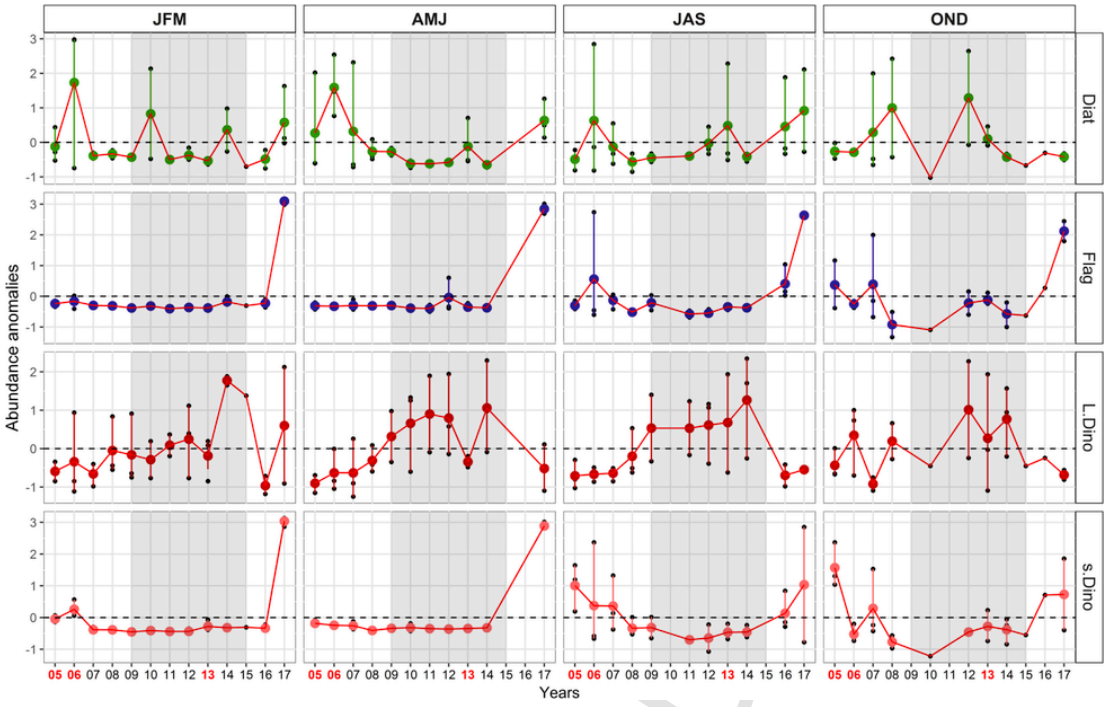

Fig. 7. 2005–2017 standardized anomaly variations of diatom (Diat), microflagellate (Flag), large dinoflagellate (L.Dino) and small dinoflagellate (s.Dino) lifeforms. Annual mean anomalies (colored points) were computed from monthly anomalie values (black points) for winter (JFM), spring (AMJ), summer (JAS) and fall (OND). Shaded area corresponded to (P_2) wet period. The years reported in the literature as they hosted intense wintering deep mixing in Ligurian Sea were indicated in bold red (ref(Heimbürger et al., 2013; Marty and Chiavérini, 2010; Pasqueron de Fommervault et al., 2015):). (For interpretation of the references to color in this figure legend, the reader is referred to the Web version of this article.)

microflagellate and small dinoflagellate abundances showed significant correlation in all seasons except in spring, despite a maximum abundance found in spring 2017 for both of them (+2.84 and + 2.87, respectively). With an exception for summer showing negative anomalies during rainy periods, no clear impact of wet period (P_2) was observed on abundances for both microflagellates and small dinoflagellates. Large and small dinoflagellate also showed a significant negative correlation during spring and summer (rho = −0.62 and −0.74). Finally, microflagellate and diatom variations showed significant positive correlation during winter (rho = 0.58).

4. Discussion

Located in a deep convection area and nearby a large agglomeration, the semi-enclosed Toulon Bay was relevant to investigate the evolution of Mediterranean marine coastal systems confronted to both climatic and anthropogenic perturbations. The monitoring of plankton in Toulon Bay was already used to study annual variability of zooplankton (Jamet et al., 2001; Richard and Jamet, 2001), microphytoplankton (Boge et al., 2006; Jamet et al., 2005; Rossi and Jamet, 2009) and pico-nanophytoplankton (Delpy et al., 2018) as well as to identify local water indicators of anthropogenic pressure (Serranito et al., 2016). By using long-term time series, the present study focuses on decadal variability (2005–2017) of the microphytoplankton community structure, to evaluate the impact of local and large-scale perturbations on coastal systems.

4.1. Microphytoplankton assemblage features

Previously cited in 1999–2000 (Jamet et al., 2005) and 2006–2007 (Rossi and Jamet, 2009) annual cycles in Toulon Bay, representative taxa selected were also characteristic of the coastal NW Mediterranean basin. Abundant diatoms such as *Chaetoceros* spp., *Thalasionema* spp. or *Pseudonitzschia* spp. were, in agreement with typical blooming genera, dominant in deep convections areas (Siokou-Frangou et al., 2010). Although it remained less frequently reported, selective dinoflagellate taxa such as *C. furca, P. micans*, *Gymnodinium* spp., or *Protoperidinium* spp. were commonly associated with summer oligotrophic period (Gómez and Gorsky, 2003) and particularly in shallow anthropized areas (Garrido et al., 2014; Vila and Maso, 2005). It should be noticed that among dinoflagellate representative taxa, five were reported as potentially toxic (*i.e. D. acuminata, P. micans*, *Alexandrium* spp., *Gonyaulax* spp., and *Gymnodinium* spp.) (Faust and Gulledge, 2002; Ignatiades and Gotsis-Skretas, 2010; Mohamed, 2018).

4.2. Drivers of changes

Asynchronous qualitative and quantitative changes in microphytoplankton communities were detected during the 2005–2017 period. A significant increase of wintering rainfall rate from late 2008 associated with a catastrophic change in salinity was followed during the next spring by the most important change among representative communities according to chronological clustering (Figs. 2 and 3). It should be noticed that the accuracy of change points is a well-known issue in regime shift studies, as it depends on the length and regularity of time-series used. Hence, the absence of data during most of 2015 led to the detection of the second change point from the end of 2015, rather than during the expecting previous spring. Investigations on total microphytoplankton abundance revealed higher values during dry periods, *i.e.* from 2005 to late spring 2006 which coincide with major wintering deep mixing events reported in Ligurian Basin (Heimbürger et al., 2013; Marty and Chiavérini, 2010) and during spring 2016 to the end of 2017 (Fig. 5).

Thenceforth, investigations on community changes pointed out two different aspects: (1) diatom and microflagellate taxa were mainly associated to dry periods (Table 3). Diatom community was furthermore promoted during springs following convection event in Ligurian open sea (Fig. 7). Only diatom taxa *Actinoptychus* spp. showed an association

with wet period, highlighting the wide diversity of life-strategies in diatoms as recently described by Kemp and Villareal (2018). (2) For dinoflagellate taxa, analysis identified two lifeforms involved in the main community changes: while small dinoflagellates ($<1{,}5.10^4$ μm^3) were also associated with dry periods, following microflagellate variations, the less abundant large dinoflagellate taxa ($>1{,}5.10^4$ μm^3) were favored by wet period (P_2).

These findings argued that changes in precipitation regime was the main driver of community changes during the 2005–2017 period, acting through different but superimposed processes at different scales: (1) a local wintering precipitation effect by runoff influence and (2) a regional precipitation deficit effect which mainly promoted vertical mixing.

4.3. Impact of local precipitation

4.3.1. Impacts on microphytoplancton community

In Toulon Bay, concomitant increase of rainfall regime and qualitative changes in microphytoplankton communities assumed impact of terrestrial runoff on community assemblage. This community change was first characterized by a shift in mixotrophic/heterotrophic dinoflagellate community, particularly during spring and summer (see appendix A), promoting the large size taxa ($>1{,}5.10^4\mu m^3$) at the expense of smaller ones. Such a shift in size structure of heterotrophic communities also suggested a change in the nature of available preys. As pointed out by significant positive correlations, small dinoflagellates were highly associated to small size microflagellates assuming a predator-prey relationship (appendix E). This hypothesis is in agreement with reports about trophic preference of mixotrophic and heterotrophic dinoflagellates reported in scientific literature. For instance, it was shown that abundant species belonging to the small dinoflagellate lifeform such as *Gymnodinium* spp. or *P. micans*, fed mainly on small size cryptophytes such as *Teleaulax* sp. (Jeong et al., 2010). Unlike other mixotrophic and heterotrophic dinoflagellates, armored *Protoperidinium* spp. which were found highly associated with (P_2) wet period, executed external digestion with an important range of size for its preys (Assmy and Smetacek, 2009; Buskey, 1997; Jacobson and Anderson, 1996). This extended diet included preferentially larger ones such as diatoms, dinoflagellates as well as ciliates (Jeong et al., 2010; Lee et al., 2014). Such feeding mechanisms allow them to modulate the classical predator-prey allometric ratio of 10:1 (Azam et al., 1983). *Protoperidinium* genus was furthermore considered as an important opportunistic grazer of red-tide species, involved in their reduction (Jeong and Latz, 1994). Thus, high predation impact from large heterotrophic dinoflagellates on other smaller protists such as little dinoflagellates and diatoms, as previously emphasized by Jeong et al. (2010), was consistent with the significant negative correlation found between these lifeforms during spring and winter (Fig. 7). Although it was not considered in this study, the increase of ciliate community during (P_2) wet period was suspected as low abundances of diatoms and small dinoflagellates observed seemed insufficient to support large dinoflagellate population growth. Furthermore, the widespread reported predation on ciliates from abundant large dinoflagellate *C.furca* (Ignatiades, 2012; Jeong et al., 2010; Smalley et al., 2003; Smalley and Coats, 2002) (which was highly associated to (P_2) wet period), also supported the increase of the ciliate population during (P_2) wet period. Finally, for the poorly studied *P. arcuatum*, also belonging to large dinoflagellates, mixotrophy and opportunistic nature was supported by the absence of correlation between abundance and nutrient concentration (Skejić et al., 2017).

4.3.2. Impacts on diatom community

Although diatom community was less impacted by the increase of wintering rainfall rate during P_2 than dinoflagellates (see appendix A), main diatom taxa were associated to dry periods (P_1 and P_3). Strict autotrophic siliceous diatoms are more sensitive to nutrient depletion or change in nutrient supply ratios than dinoflagellates, particularly for silicon (Si) (Anderson et al., 2002). It was assumed that diatoms were favored in Si:N:P = 16:16:1 conditions (Redfield et al., 1963) and that a variation from this ratio may result in a community shift toward non siliceous and smaller community (Cloern, 2001; Reynolds, 2006). For instance, a decrease in SI:N ratio in Bay of Brest between 1977 and 1995 due to an increase of anthropogenic nitrogen inputs from runoff, led to a limitation of the spring bloom intensity and an increase of haptophyta *Phaeocystis* sp. bloom (Chauvaud et al., 2000). Though nutrients (mainly nitrates) and organic matter as well as metallic contaminant were carried into Toulon Bay by Eygoutier River induced by heavy rain events (Nicolau et al., 2006), the relation between our increase of rainfall and nutrient supply remained unclear due to the lack of data. However, the reduction and the disappearance of the most abundant spring bloom diatom taxa as well as the silico flagellate *Dictyocha* sp. during P_2 suggested a nutrient depletion condition or a change in nutrient supply ratios. Also, as mixotrophic dinoflagellates were known to outcompete diatoms in organic nutrient conditions (Spilling et al., 2018), the change observed within the community may also suggest the impact of organic matter input from the Eygoutier River. It is interesting to note that such hypothesis contrast with the few available studies investigating the impact of freshwater runoff on phytoplankton communities in coastal northwestern subbasin due to specific trophic state conditions. For instance, from shallow Blanes Bay station (Catalan coast) rainfall events were followed by an increase of diatom, dinoflagellate or cryptophyte abundances as well as spring bloom intensity (Nunes et al., 2018). Similarly, in oligotrophic northern coastal Adriatic sea, the reduction of freshwater flow was identified as a driver of both change in phytoplanktonic composition, and reduction of total abundance during the 1986–2077 period (Aubry et al., 2012; Cabrini et al., 2012). Recently in the same region, a re-increase of the Pô river outflow observed during the 2007–2016 was followed by a reduction of coccolithophorid and by an increase in phytoflagellate biomass (Totti et al., 2019).

4.3.3. Impacts on chlorophyll a

In Toulon Bay, the absence of significant change in chlorophyll *a* concentration at the decadal scale contrast with the total microphytoplankton dynamic which followed mainly diatom variations. A significant negative correlation was furthermore found between their respective trends. As such, and although nanophytoplankton coccolithophorids were not investigated, chlorophyll *a* concentration would reflected mainly the nanophytoplankton dynamic rather than upper phytoplankton size class. As pointed out by Uitz et al. (2012), except during blooming periods, small size classes of phytoplankton (particularly nanoplankon) contributed more to chlorophyll *a* concentration than microphytoplankton in NW Mediterranean Sea. Nanophytoplankton was also known to 'overcompete' other phytoplankton classes in oligotrophic conditions (Siokou-Frangou et al., 2010), particularly due to a higher population growth rate and their ability to reduce the nutrient diffusion (Marañón, 2015). Thus, the contrasted dynamics between microphytoplancton and chlorophyll *a* also argue in favor of a shift in trophic conditions toward oligotrophy as a result of the increased rainfall rate. This shift would lead, in turn to changes from diatom and microflagellate dominance to smaller phytoplankton dominance-based system, which favored opportunistic large dinoflagellates.

4.4. Footprints from wintering deep mixings

Impact of wintering deep mixings was also observed in total microphytoplankton abundance as well as in diatom anomalies. During the early 2000s, deficit in freshwater budget caused by a low annual pre-

cipitation rate was identified as the main driver of intense convection events in the central Ligurian Sea, observed in 2005 and particularly in 2006 (Marty and Chiavérini, 2010). More recently, Coppola et al. (2018), reported at the DYFAMED point (central Ligurian Sea), a deepening of MLD during the winter 2013 suggesting a new but less intense, deep-mixing event. Concomitance between positive anomalies observed in diatom abundances during spring 2005, 2006 and 2013 (Fig. 7) and reported deep-mixings, supported the hypothesis of the influence of regional mixing events on local microphytoplankton. Likewise, high salinity and dry conditions observed in 2005–2007 period (P_1) were in agreement with the increase of salinity and the deficit in precipitation pointed out from the early 2000's in Ligurian Basin (Marty and Chiavérini, 2010). It would confirm the role of salinity as a powerful indicator of large scale process in NW Mediterranean Sea (Somot et al., 2006). However, no coherent change or trend was identified in water temperature in Toulon Bay during the 2005–2017 period (Fig. 3c). Changes in water temperature has been also suspected as the main hydrologic feature related to climate change and large scale processes in NW Mediterranean Sea (Goffart et al., 2015, 2002; Trigo and Davies, 2000; Vargas-Yáñez et al., 2010, 2008). We assumed that the absence of significant variability of water temperature in Toulon Bay during wintering deep mixing events (*i.e.* decrease of Sea Surface Temperature) (Marty and Chiavérini, 2010) was probably due to both low water circulation into the bay and the impact of the local northern cold wind (Mistral). Second salty and dry period observed from early 2015 was also followed in winter and spring 2017 by an abrupt increase in total microphytoplankton abundance as well as positive anomalies in diatom and particularly in autotrophic microflagellates. Similarly to the beginning of 2000's, as low precipitation rate was observed in other meteorological stations around the Ligurian basin (*i.e.* Marseille, Nice and Calvi, see appendix F for details), a new freshwater deficit at a regional scale was suspected, leading to a potential new intense mixing event in 2017. Due to the absence of current reports, further investigations on late 2010s would be necessary to confirm occurrence of such a new deep mixing in Ligurian Sea as suggested by our biological responses and abiotic conditions.

From the above discussion points, we produced a simplified model (Fig. 8) about the impact of rainfall on long term microphytoplankton dynamic in Toulon Bay, through two main mechanisms: 1) regional deep mixing events triggered by rainfall deficit, is the main fertilization driver of Toulon Bay, by shaping interannual variations of microflagellate and particularly diatom spring bloom intensity. 2) the impact of wintering runoff intensification which promote smaller primary producer and lead to substantial changes in upper trophic levels such as in heterotrophic protists.

4.5. Community variability during dry periods

Although both dry and salty periods *i.e.* 2005–2008 (P_1) and 2015–2017 (P_3) shared assemblages dominated by diatoms and smaller microflagellate taxa, numerous taxa were associated with only one of them. Thus, P_1 appeared mainly associated with diatoms and some heterotrophic flagellates whereas P_3 was characterized by smaller autotrophic microflagellate (mainly cryptophyte species *H.fusiformis*) as shown by $IndVal_g$ (Table 3). Such pattern characterizing a second alternation in primary producer nature may be driven by another notable variability in nutrient supply during dry period. For instance, as the nutrient content of deep layers showed a decadal variability (Pasqueron de Fommervault et al., 2015), variations in the composition of the nutrients provided by wintering mixing events could be considered. Likewise, presence of instabilities from Northern Current in Toulon Bay (Guihou et al., 2013) could represent another local factor of nutrient enrichment, fueling punctual blooms (Casella et al., 2014)

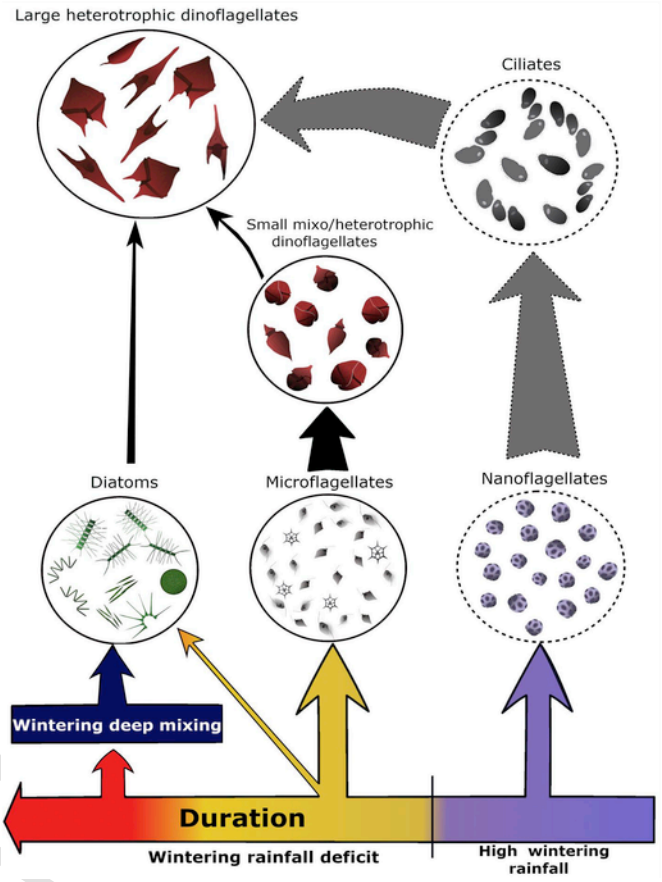

Fig. 8. Simplified scenario of microphytoplanktonic ecosystem functioning in Toulon Bay related to wintering rainfall variability. Arrows indicated highlighted (full black) and suspected (dashed grey) trophic relations between investigated (full circles) and not-investigated (dashed circles) planktonic communities. Arrow thickness indicated the strength of relation supported by evidences. Rainy winters seemed favor small autotrophic cells (nanoflagellates) leading to important increase of large heterotrophic dinoflagellates sustained by ciliates. Dry winters promoted slightly abundant diatom and especially micro-flagellate communities which were highly correlated with small mixotrophic dinoflagellates. Both diatoms and small dinoflagellates may also be predated by larger dinoflagellates (mainly *Protoperidinium* spp.). Finally, rainfall deficit over several years was assumed as a driver of winter deep mixing at regional scale which triggered intense diatom spring blooms in Toulon Bay.

as pointed out in the French Riviera (Sammari et al., 1995; Taupier-Letage and Millot, 1986).

5. Conclusion

Using long-term monitoring time-series (2005–2017), the present study provides new insights on decadal microphytoplancton variations in a semi-enclosed and anthropized area, highlighting cell size as an important descriptor of structure composition changes. Our data showed that precipitations were a keystone of microphytoplankton dynamics as it was involved in assemblage variations and bloom intensity: 1) Local wintering runoff was suspected to modify water nutrient supply ratio to the benefit of smaller and non-siliceous autotrophic communities such as nanophytoplankton and promoting opportunistic heterotrophic protists. 2) Regional rainfall deficit was identified as an important conditioning factor for wintering deep mixings in Ligurian Basin, and a key regulator of intense diatom and microflagellate spring blooms in the northern coast. Further investigations might be necessary to highlight suspected impacts of riverine on nutrient concentrations as well as consequences in upper trophic levels such as copepods. Furthermore, our results support the idea that microphytoplankton composition with an emphasis on size structure can be used as BQE regarding

of WFD and MSFD (Marine Strategy Framework Directory, 2008/56/EC) policies as it succeeds to detect substantial changes in plankton ecosystem functioning while chlorophyll *a* concentration failed. As a result, we highlighted the importance to consider the size of dinoflagellate as a hallmark of deep changes in trophic state of coastal ecosystems. Finally, in agreement with Nunes et al. (2018), this work confirms the need of a higher consideration of rainfall variations for future predictions related to climate change in the frame of coastal management as it represents a major stressor for ecosystems confronted to high human pressures.

Declaration of interests

None.

Author contributions

B.S. conceived this study, designed figures, performed analysis and wrote the paper. D.J., J-L.J, N.R., and B.S. participated to the biological data collection. D.J. with N.R. realized the biological sampling expertise. B.S. also gathered abiotic data and other biological traits with D.J. and N.R.

D.J. and J-L.J. conceived the global framework of the project and were responsible to the setting up of plankton monitoring in Toulon Bay. All authors agreed on the final version of the manuscript.

Fundings

This study was financed by an in-house funding from the EBMA (Marine Ecology and Biology) research team (PROTEE laboratory EA 3819, University of Toulon, France).

Acknowledgements

We would like to thank Dr Daniel Petit for his helpful comments, Dr Charlotte Dubois and Dr Luce Perié for the proofreading of the manuscript and their valuable advices. This research did not receive any specific grant from funding agencies in the public, commercial, or not-for-profit sectors.

Appendix A.

Summary of the non-parametric pairwise ANOSIM analysis between extracted periods (P_1, P_2 et P_3, respectively) for total microphytoplankton community (Total) and for diatoms, dinoflagellates and microflagellates, using respective log-chord distance matrix, and for each season independently (JFM, AMJ, JAS, and OND, were for winter, spring, summer and fall, respectively). Analysis returned "R" values, ranged between −1 and 1, indicating the degree of differences between periods. High positive values suggested more similarities within the same period than between periods. Significance of differences between periods (blue bold cases) was performed by bootstrapping using 10′000 random permutations with Bonferroni corrections.

	JFM		AMJ	
Total	**0.23**		**0.40**	
	P_2	P_3	P_2	P_3
P_1	**0.24**	0.15	**0.48**	0.0
P_2		0.05		**0.3**
Diatoms	**0.15**		**0.18**	
	P_2	P_3	P_2	P_3
P_1	**0.27**	0.02	**0.29**	-0.
P_2		-0.02		-0.
Dinoflagellates	0.01		**0.37**	
	P_2	P_3	P_2	P_3
P_1	0.07	0	**0.35**	0.1
P_2		0.12		**0.5**
Microflagellates	0.02		**0.23**	
	P_2	P_3	P_2	P_3
P_1	-0.03	0.06	**0.25**	0.0
P_2		0.09		0.2

Appendix B.

Details and summary for biovolume computation of selected taxa. For each taxa, geometric **shape** and **formula** with respective dimensions (**Dim1**, **Dim2** and **Dim3**) were reminded. For measured dimensions (**o**), **n1** indicate the number of sampling used. For lacking dimension (**i**), interpolations were performed using linear regression ($y = ax$) between the target (**y**) and reference dimension (**x**) from Olenina et al. (2006) dataset. For each lacking dimension, number of values used (**n2**), the slope (**a**) and respective $\mathbf{r^2}$ with pvalue (* <0.05; ** <0.01; *** <0.001.) were specified. For complex shapes (*i.e. Ceratium* genera), final biovolum was obtained by adding the volume of different parts.

				Dimensions			
Class	Taxa	Shape	V formula	n1	D1		D2
Diatoms	A.gla	cone + half sphere	$\pi/12^* D2^2 *(D1/2 + D2)$	9	i	Height	o
	Act	cylindre	$\pi/4^*D2^{2*} D1$	38	i	Length	o
	B.del	cylindre	$\pi/4^*D2^{2*} D1$	16	i	Length	o
	C.clo	2 cones	$\pi/12^* D2^2 *D1$	63	i	Length	o
	Chae	elliptic prism	$\pi/4^*D1^*D2^*D3$	162	o	Length	o
	Cos	cylindre	$\pi/4^*D2^{2*} D1$	72	i	Length	o
	Cyc	cylindre	$\pi/4^*D2^{2*} D1$	102	i	Length	o
	D.fra	cylindre	$\pi/4^*D2^{2*} D1$	26	o	Length	o
	F.cyl	elliptic prism	$\pi/4^*D1^*D2$	3	o	Length	o

	Gui	cylindre	$\pi/4*D2^{2}*$ D1	63	i	Length
	Gyros	prism on parallelo-gram base	0,5*D1*D2*D3	14	o	Height
	H.hau	cylindre	$\pi/4*D2^{2}*$ D1	16	o	Length
	L.dan	cylindre	$\pi/4*D2^{2}*$ D1	45	o	Length
	L.gra	gom-phonemoid	(D1*D3)/4	23	o	Height
			*(D1 + ((π/4)-1)*D3)			
			*asin(D2/(2*D1))		o	Height
	Lio	cylindre	$\pi/4*D2^{2}*$ D1	3	o	Length
	Nav	elliptic prism	π/4*D1*D2*D3	41	o	Length
	Nit	prism on parallelo-gram base	0,5*D1*D2*D3	31	o	Height
	P.del	prism on parallelo-gram base	0,5*D1*D2*D3	63	o	Height
	P.ser	prism on parallelo-gram base	0,5*D1*D2*D3	19	o	Height
	Pseu	prism on parallelo-gram base	0,5*D1*D2*D3	6	o	Height
	Pleu	prism on parallelo-gram base	0,5*D1*D2*D3	10	o	Height
	Rhi	cylindre	$\pi/4*D2^{2}*$ D1	32	o	Length
	S.cos	cylindre	$\pi/4*D2^{2}*$ D1	13	o	Length
	Tnema	paral-lelepiped	D1*D2*D3	97	o	Height
	Tsira	cylindre	$\pi/4*D2^{2}*$ D1	16	o	Length
Dinofla-gel-lates	Ach	prolate spheroid	$\pi/6*D2^{2}*D1$	49	o	Length
	Alei	prolate spheroid	$\pi/6*D2^{2}*D1$	34	i	Length
	Amp	ellipsoïd	π/6*D1*D2*D3	15	i	Length
	Amy	cone + half sphere	$\pi/12*$ $D2^{2}$ *(D1/2 + D2)	10	o	Height
	C.fur	prolate spheroid	$\pi/6*D2^{2}*D1$	43	o	Length
		2 * cones	2* ($\pi/12*$ $D2^{2}$ *D1)		o	Height
		cylindre	$\pi/4*D2^{2}*$ D1		o	Length
	C.fus	2 cones	$\pi/12*$ $D2^{2}$ *D1	39	o	Length
	C.pen	prolate spheroid	$\pi/6*D2^{2}*D1$	4	o	Length
		2 * cones	$\pi/12*$ $D2^{2}$ *D1		o	Length
		cylindre	$\pi/4*D2^{2}*$ D1		o	Length
	Cor	2 cones	$\pi/12*D1*D2^{2}$	11	o	Length
	D.acu	ellipsoïd	π/6*D1*D2*D3	21	i	Length
	Gon	sphere	$\pi/6*D2^{3}$	17		o
	Gony	cone + half sphere	$\pi/12*$ $D2^{2}$ *(D1/2 + D2)	24	i	Height
	Gym	ellipsoïd	π/6*D1*D2*D3	217	i	Length
						o
	Gyrod	ellipsoïd	π/6*D1*D2*D3	7	o	Length
	Oiy	prolate spheroid	$\pi/6*D1^{2}*D1$	36	o	Length
	P.arc	prolate spheroid	$\pi/6*D1^{2}*D1$	47	o	Length
	P.div	2 cones	$\pi/12*D1*D2^{2}$	16	o	Length
	P.mic	prolate spheroid	$\pi/6*D2^{2}*D1$	44	o	Length
	P.pel	2 cones	$\pi/12*D1*D2^{2}$	12	o	Length
	P.pen	2 cones	$\pi/12*D1*D2^{2}$	10	o	Length
	Prot.L	2 cones	$\pi/12*D1*D2^{2}$	14	o	Length
	Prot.s	2 cones	$\pi/12*D1*D2^{2}$	18	o	Length
	Scri	prolate spheroid	$\pi/6*D2^{2}*D1$	68	o	Length
Flagel-lates	Chla	sphere	$\pi/6*D1^{3}$	15		o
	Chlo	sphere	$\pi/6*D1^{3}$	42		o
	Chro	sphere	$\pi/6*D1^{3}$	3		o
	Dict	sphere	$\pi/6*D1^{3}$	65		o
	H.fus	prolate spheroid	$\pi/6*D2^{2}*D1$	65	o	Length
	Hemi	cone + half sphere	$\pi/12*$ $D2^{2}$ *(D1/2 + D2)	8	i	Height
	Het	cone + half sphere	$\pi/12*$ $D2^{2}$ *(D1/2 + D2)	13	o	Height
	Leu	cone + half sphere	$\pi/12*$ $D2^{2}$ *(D1/2 + D2)	26	o	Height
	Rho	cone + half sphere	$\pi/12*$ $D2^{2}$ *(D1/2 + D2)	7	o	Height
	Tetra	prolate spheroid	$\pi/6*D2^{2}*D1$	17	o	Length

Appendix C.

Mean difference in dinoflagellate species abundances between P2 and P1 (left panel) and between P3 and P2 (right panel) with respect to their mean cell biovolume. X axis was expressed in log transformed data to linearize the relation. Full red lines with confident interval (shaded areas) were for significant linear regressions on log transformed biovolums, used to evaluate the threshold defining life-forms. Red dotted vertical line indicated when the linear model displayed a change in sign in the difference, leading to an average biovolume threshold at $1{,}5.10^{4}$ μm^{3}.

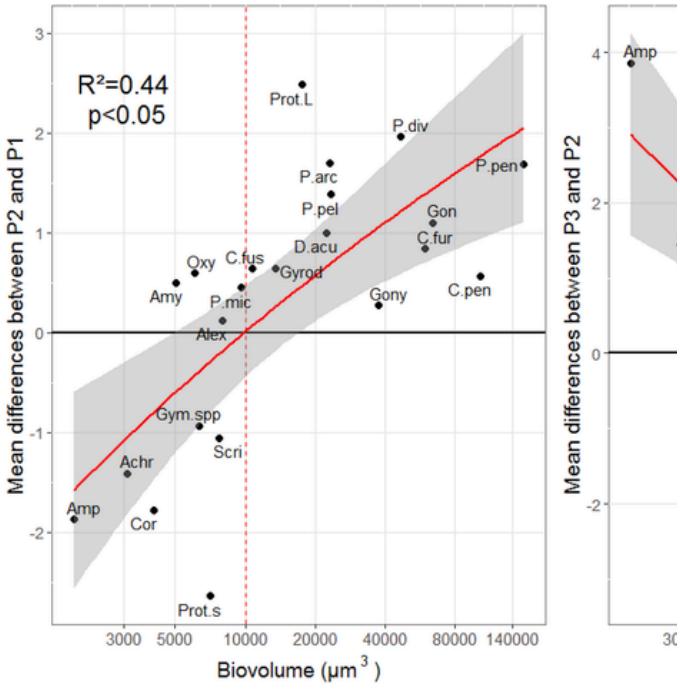

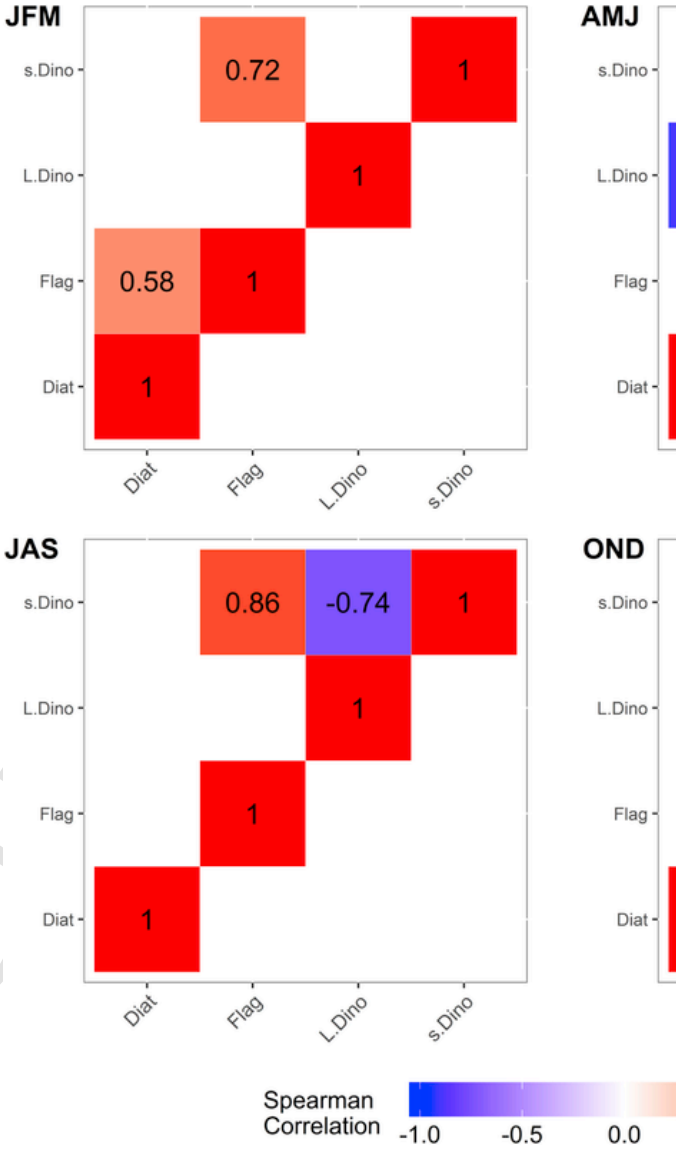

Appendix D. Corresponding date ranges for "environmental" and "micro-phytoplankton" datasets partitioning

	P_1	P_2	P_3
Environmental	Feb-2006 – Nov - 2008	Dec-2008- Feb-2015	Mar-2015 – Nov-2017
Micro-phyto-plankton	Jan-2005 – Mar 2009	Apr-2009 – Jan-2015	Dec-2015 – Nov-2017

Appendix E.

Lifeform correlograms of 2005–2017 mean annual anomalie variations during winter (JFM). spring (AMJ), summer (JAS) and fall (OND). Color blocks and values indicated Spearman's rho correlation. Only significant values (pval < 0.05) were displayed.

Appendix F.

2005–2018 standardized anomalies of precipitation rate describing variations from monthly mean values, from 3 météorological coastal stations around the Ligurian Basin: Calvi (42°31′46′′N; 8°47′29′′E), Nice (43°38′56′′N; 7°12′32′′E), Marseille (43°18′20′′N; 5°23′40′′E). For each station, panel showed anomalies (grey area), loess regression (α parameter = 0.3) (black line) to summarize the trend, and vertical dotted line precised significant rainfall rate changes observed in Toulon bay. Discontinuity in the trend was related to lack of data. Similar pattern of variability was observed in each station: globally, as highlighted in Toulon Bay, 2009-early 2015 period was characterized by an increase of precipitation while 2005–2008 and 2015–2017 periods were marked by a relative droughtness condition, confirming coherent meteorological pattern at the basin scale.

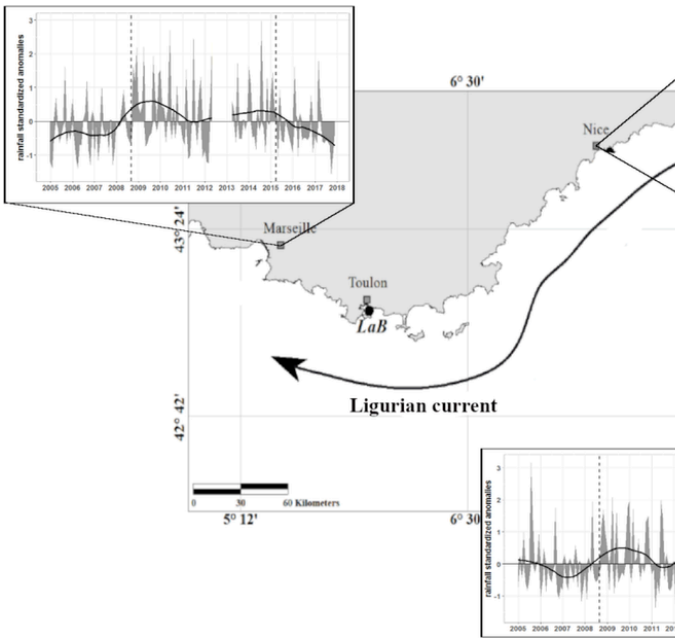

References

Adolf, J.E., Yeager, C.L., Miller, W.D., Mallonee, M.E., Harding, L.W., 2006. Environmental forcing of phytoplankton floral composition, biomass, and primary productivity in Chesapeake Bay, USA. Estuar. Coast Shelf Sci. 67, 108–122 https://doi.org/10.1016/j.ecss.2005.11.030.

Aminot, A., Kérouel, R., 2007. Méthodes en flux continu. In: Dosage Automatique Des Nutriments Dans Les Eaux Marines, Méthodes D'analyse En Milieu Marin. Ifremer.

Aminot, A., Kérouel, R., 2004. Hydrologie des écosystèmes marins: paramètres et analyses, Editions Ifremer. In: Méthodes d'analyse en milieu marin. Ifremer.

Anderson, D.M., Glibert, P.M., Burkholder, J.M., 2002. Harmful algal blooms and eutrophication:nutrient sources, composition and comsequences. Estuaries 25, 704–726.

Anderson, M.J., 2001. A new method for non-parametric multivariate analysis of variance. Austral Ecol. 26, 32–46.

Assmy, P., Smetacek, V., 2009. Algal blooms. Encyclopedia of Microbiology. Elsevier, Oxford, 27–41 https://doi.org/10.13140/2.1.4051.8081.

Aubry, F.B., Cossarini, G., Acri, F., Bastianini, M., Bianchi, F., Camatti, E., De Lazzari, A., Pugnetti, A., Solidoro, C., Socal, G., 2012. Plankton communities in the northern Adriatic Sea: patterns and changes over the last 30 years. Estuar. Coast Shelf Sci. 115, 125–137 https://doi.org/10.1016/j.ecss.2012.03.011.

Azam, F., Fenchel, T., Field, J., Gray, J., Meyer-Reil, L., Thingstad, F., 1983. The ecological role of water-column microbes in the sea. Mar. Ecol. Prog. Ser. 10, 257–263 https://doi.org/10.3354/meps010257.

Barton, A.D., Pershing, A.J., Litchman, E., Record, N.R., Edwards, K.F., Finkel, Z.V., Kiørboe, T., Ward, B.A., 2013. The biogeography of marine plankton traits. Ecol. Lett. 16, 522–534 https://doi.org/10.1111/ele.12063.

Basu, S., Mackey, K., 2018. Phytoplankton as key mediators of the biological carbon pump: their responses to a changing climate. Sustainability 10, 869 https://doi.org/10.3390/su10030869.

Belin, C., Daniel, A., Gauthier, E., Lampert, L., Neaud-Masson, N., Soudant, D., Derolez, V., 2017. REPHY dataset - French Observation and Monitoring program for Phytoplankton and Hydrology in coastal waters. 1987-2016 Metropolitan data. In: https://doi.org/10.17882/47248.

Berland, B., Maestrini, S., Grzebyk, D., Thomas, P., 1995. Recent aspects of nutrition in the dinoflagellate Dinophysis cf. acuminata. Aquat. Microb. Ecol. 9, 191–198 https://doi.org/10.3354/ame009191.

Bockstahler, K.R., Coats, D.W., 1993. Grazing of the mixotrophic dinoflagellate Gymnodinium sanguineum on ciliate populations of Chesapeake Bay. Mar. Biol. 116, 477–487 https://doi.org/10.1007/BF00350065.

Boge, G., Jean, N., Jamet, J.-L., Jamet, D., Richard, S., 2006. Seasonal changes in phosphatase activities in Toulon Bay (France). Mar. Environ. Res. 61, 1–18 https://doi.org/10.1016/j.marenvres.2005.03.002.

Boyce, D.G., Frank, K.T., Leggett, W.C., 2015. From mice to elephants: overturning the 'one size fits all' paradigm in marine plankton food chains. Ecol. Lett. 18, 504–515 https://doi.org/10.1111/ele.12434.

Brahim, M.B., Feki, M., Feki-Shnoum, W., Mahfoudi, M., Hamza, A., 2015. Factor driving heterotrophic dinoflagellate in relation to environment conditions in Kerkennah Islands (eastern coast of Tunisa). J. Coast. Life Med. 3, 686–690 https://doi.org/10.12980/jclm.3.2015j5-85.

Brewin, R.J.W., Hardman-Mountford, N.J., Lavender, S.J., Raitsos, D.E., Hirata, T., Uitz, J., Devred, E., Bricaud, A., Ciotti, A., Gentili, B., 2011. An intercomparison of bio-optical techniques for detecting dominant phytoplankton size class from satellite remote sensing. Remote Sens. Environ. 115, 325–339 https://doi.org/10.1016/j.rse.2010.09.004.

Buric, Z., Caput Mihalic, K., Cetinic, I., Ciglenecki, I., Caric, M., Vilicic, D., Cosovic, B., 2009. Occurrence of the rare microflagellates prorocentrum arcuatum issel and hermesinum adriaticum zacharias in the marine lake rogoznica (eastern adriatic coast). Acta Adriat. 1, 31–44.

Buskey, E., 1997. Behavioral components of feeding selectivity of the heterotrophic dinoflagellate Protoperidinium pellucidum. Mar. Ecol. Prog. Ser. 153, 77–89 https://doi.org/10.3354/meps153077.

Cabrini, M., Fornasaro, D., Cossarini, G., Lipizer, M., Virgilio, D., 2012. Phytoplankton temporal changes in a coastal northern Adriatic site during the last 25 years. Estuar. Coast Shelf Sci. 115, 113–124 https://doi.org/10.1016/j.ecss.2012.07.007.

Casella, E., Tepsich, P., Couvelard, X., Caldeira, R.M.A., Schroeder, K., 2014. Ecosystem dynamics in the Liguro-Provençal Basin: the role of eddies in the biological production. Mediterr. Mar. Sci. 15, 274–286.

Chauvaud, L., Jean, F., Ragueneau, O., Thouzeau, G., 2000. Long-term variation of the Bay of Brest ecosystem:benthic-pelagic coupling revisited. Mar. Ecol. Prog. Ser. 200, 35–48 https://doi.org/10.3354/meps200035.

Cid, A., Abalde, J., Herrero, C., 1992. High yield mixotrophic cultures of the marine microalga Tetraselmis suecica (Kylin) Butcher (Prasinophyceae). J. Appl. Phycol. 4, 31–37 https://doi.org/10.1007/BF00003958.

Cloern, J.E., 2001. Our evolving conceptual model of the coastal eutrophication problem. Mar. Ecol. Prog. Ser. 210, 223–253.

Cloern, J.E., Abreu, P.C., Carstensen, J., Chauvaud, L., Elmgren, R., Grall, J., Greening, H., Johansson, J.O.R., Kahru, M., Sherwood, E.T., Xu, J., Yin, K., 2016. Human activities and climate variability drive fast-paced change across the world's estuarine-coastal ecosystems. Glob. Chang. Biol. 22, 513–529 https://doi.org/10.1111/gcb.13059.

Cloern, J.E., Dufford, R., 2005. Phytoplankton community ecology: principles applied in San Francisco Bay. Mar. Ecol. Prog. Ser. 285, 11–28.

Coppola, L., Legendre, L., Lefevre, D., Prieur, L., Taillandier, V., Diamond Riquier, E., 2018. Seasonal and inter-annual variations of dissolved oxygen in the northwestern Mediterranean Sea (DYFAMED site). Prog. Oceanogr. 162, 187–201 https://doi.org/10.1016/j.pocean.2018.03.001.

Costanza, R., de Groot, R., Sutton, P., van der Ploeg, S., Anderson, S.J., Kubiszewski, I., Farber, S., Turner, R.K., 2014. Changes in the global value of ecosystem services. Glob. Environ. Chang. 26, 152–158 https://doi.org/10.1016/j.gloenvcha.2014.04.002.

Physical influences on marine ecosystem dynamics. In: Cullen, J.J., Franks, P.J., Karl, D.M., Longhurst, A. (Eds.), Biological-Physical Interactions in the Sea, the Sea the Global Coastal Ocean. Harvard Univ. Press, Cambridge, Mass, pp. 2002. 297–336.

Cushing, D.H., 1989. A difference in structure between ecosystems in strongly stratified waters and in those that are only weakly stratified. J. Plankton Res. 11, 1–13.

d'Ortenzio, F., Ribera d'Alcalà, M., 2009. On the trophic regimes of the Mediterranean Sea: a satellite analysis. Biogeosciences 6, 139–148.

De Cáceres, M., Legendre, P., 2009. Associations between species and groups of sites indices and statistical inference. Ecology 12, 3566–3574.

De Cáceres, M., Legendre, P., Moretti, M., 2010. Improving indicator species analysis by combining groups of sites. Oikos 119, 1674–1684 https://doi.org/10.1111/j.1600-0706.2010.18334.x.

de Groot, R., Brander, L., van der Ploeg, S., Costanza, R., Bernard, F., Braat, L., Christie, M., Crossman, N., Ghermandi, A., Hein, L., Hussain, S., Kumar, P., McVittie, A., Portela, R., Rodriguez, L.C., ten Brink, P., van Beukering, P., 2012. Global estimates of the value of ecosystems and their services in monetary units. Ecosyst. Serv. 1, 50–61 https://doi.org/10.1016/j.ecoser.2012.07.005.

Delpy, F., Serranito, B., Jamet, J.-L., Grégori, G., Le Poupon, C., Jamet, D., 2018. Pico- and nanophytoplankton dynamics in two coupled but contrasting coastal bays in the NW Mediterranean sea (France). Estuar. Coasts https://doi.org/10.1007/s12237-018-0412-9.

Devlin, M., Best, M., Coates, D., Bresnan, E., O'Boyle, S., Park, R., Silke, J., Cusack, C., Skeats, J., 2007. Establishing boundary classes for the classification of UK marine waters using phytoplankton communities. Mar. Pollut. Bull. 55, 91–103 https://doi.org/10.1016/j.marpolbul.2006.09.018.

Dodson, A.N., Thomas, W.H., 1964. Concentrating plankton in a gentle fashion. Limnol. Oceanogr. 9, 455–456.

Ducklow, H.W., Doney, S.C., Steinberg, D.K., 2009. Contributions of long-term research and time-series observations to marine ecology and biogeochemistry. Annu. Rev. Mar. Sci. 1, 279–302 https://doi.org/10.1146/annurev.marine.010908.163801.

Dufrene, M., Legendre, P., 1997. Species assemblages and indicator species: the need for a flexible asymmetrical approach. Journal. Monogr. 67, 345–366.

Dufresne, C., Duffa, C., Rey, V., 2014. Wind-forced circulation model and water exchanges through the channel in the Bay of Toulon. Ocean Dynam. 64, 209–224 https://doi.org/10.1007/s10236-013-0676-3.

Faust, M.A., Gulledge, R.A., 2002. Identifying harmful marine dinoflagellates. Contrib. U. S. Natl. Herb. 4, 1–144.

Flynn, K.J., Stoecker, D.K., Mitra, A., Raven, J.A., Glibert, P.M., Hansen, P.J., Graneli, E., Burkholder, J.M., 2013. Misuse of the phytoplankton-zooplankton dichotomy: the need to assign organisms as mixotrophs within plankton functional types. J. Plankton Res. 35, 3–11 https://doi.org/10.1093/plankt/fbs062.

Garrido, M., Koeck, B., Goffart, A., Collignon, A., Hecq, J.-H., Agostini, S., Marchand, B., Lejeune, P., Pasqualini, V., 2014. Contrasting patterns of phytoplankton assemblages in two coastal ecosystems in relation to environmental factors (corsica, NW Mediterranean sea). Diversity 6, 296–322 https://doi.org/10.3390/d6020296.

Goffart, A., Hecq, J.-H., Legendre, L., 2015. Drivers of the winter–spring phytoplankton bloom in a pristine NW Mediterranean site, the Bay of Calvi (Corsica): a long-term study (1979–2011). Prog. Oceanogr. 137, 121–139 https://doi.org/10.1016/j.pocean.2015.05.027.

Goffart, A., Hecq, J.-H., Legendre, L., 2002. Changes in the development of the winter-spring phytoplankton bloom in the Bay of Calvi (NW Mediterranean) over the last two decades: a response to changing climate?. Mar. Ecol. Prog. Ser. 236, 45–60.

Gómez, F., Gorsky, G., 2003. Annual microplankton cycles in villefranche bay, Ligurian Sea, NW mediterranean. J. Plankton Res. 25, 323–339.

Grover, J.P., 1989. Influence of cell shape and size on algal competitive ability. J. Phycol. 25, 402–405.

Guidi, L., Chaffron, S., Bittner, L., Eveillard, D., Larhlimi, A., Roux, S., Darzi, Y., Audic, S., Berline, L., Brum, J.R., Coelho, L.P., Espinoza, J.C.I., Malviya, S., Sunagawa, S., Dimier, C., Kandels-Lewis, S., Picheral, M., Poulain, J., Searson, S., Stemmann, L., Not, F., Hingamp, P., Speich, S., Follows, M., Karp-Boss, L., Boss, E., Ogata, H., Pesant, S., Weissenbach, J., Wincker, P., Acinas, S.G., Bork, P., de Vargas, C., Iudicone, D., Sullivan, M.B., Raes, J., Karsenti, E., Bowler, C., Gorsky, G., 2016. Plankton networks driving carbon export in the oligotrophic ocean. Nature https://doi.org/10.1038/nature16942.

Guihou, K., Marmain, J., Ourmières, Y., Molcard, A., Zakardjian, B., Forget, P., 2013. A case study of the mesoscale dynamics in the North-Western Mediterranean Sea: a combined data–model approach. Ocean Dynam. 63, 793–808 https://doi.org/10.1007/s10236-013-0619-z.

Hansen, B., Bjornsen, P.K., Hansen, P.J., 1994. The size ratio between planktonic predators and their prey. Limnol. Oceanogr. 39, 395–403.

Hansen, G., Moestrup, , Roberts, K.R., 1996. Fine structural observations on Gonyaulax spinifera (Dinophyceae), with special emphasis on the flagellar apparatus. Phycologia 35, 354–366 https://doi.org/10.2216/i0031-8884-35-4-354.1.

Harding, L.W., Gallegos, C.L., Perry, E.S., Miller, W.D., Adolf, J.E., Mallonee, M.E., Paerl, H.W., 2016. Long-term trends of nutrients and phytoplankton in chesapeake bay. Estuar. Coasts 39, 664–681 https://doi.org/10.1007/s12237-015-0023-7.

Heimbürger, L.-E., Lavigne, H., Migon, C., D'Ortenzio, F., Estournel, C., Coppola, L., Miquel, J.-C., 2013. Temporal variability of vertical export flux at the DYFAMED time-series station (Northwestern Mediterranean Sea). Prog. Oceanogr. 119, 59–67 https://doi.org/10.1016/j.pocean.2013.08.005.

Hillebrand, H., Dürselen, C.-D., Kirschtel, D., Pollingher, U., Zohary, T., 1999. Biovolume calculation for pelagic and benthic microalgae. J. Phycol. 35, 403–424.

Höglander, H., Karlson, B., Johansen, M., Walve, J., Andersson, A., 2013. Overview of coastal phytoplankton indicators and their potential use in Swedish waters. WATERS Report Series 5, 87.

Ignatiades, I., 2015. Redefinition of cell size classification of phytoplankton – a potential tool for improving the quality and assurance of data interpretation. Mediterr. Mar. Sci. 17, 56–64.

Ignatiades, L., 2012. Mixotrophic and heterotrophic dinoflagellates in eutrophic coastal waters of the Aegean Sea (eastern Mediterranean Sea). Bot. Mar. 55, 39–48 https://doi.org/10.1515/bot-2012-0096.

Ignatiades, L., Gotsis-Skretas, O., 2010. A review on toxic and harmful algae in Greek coastal waters (E. Mediterranean sea). Toxins 2, 1019–1037 https://doi.org/10.3390/toxins2051019.

Jaanus, A., Toming, K., Hällfors, S., Kaljurand, K., Lips, I., 2009. Potential phytoplankton indicator species for monitoring Baltic coastal waters in the summer period. Hydrobiologia 629, 157–168 https://doi.org/10.1007/s10750-009-9768-y.

Jacobson, D.M., Anderson, D.M., 1996. Widespread phagocytosis of ciliates and other protists by marine mixotrophic and heterotrophic thecate dinoflagellates. J. Phycol. 32, 279–285 https://doi.org/10.1111/j.0022-3646.1996.00279.x.

Jamet, J.L., Bogé, G., Richard, S., Geneys, C., Jamet, D., 2001. The zooplankton community in bays of Toulon area (northwest Mediterranean Sea, France). Hydrobiologia 457, 155–165.

Jamet, J.-L., Jean, N., Bogé, G., Richard, S., Jamet, D., 2005. Plankton succession and assemblage structure in two neighbouring littoral ecosystems in the north-west Mediterranean Sea. Mar. Freshw. Res. 56, 69 https://doi.org/10.1071/MF04102.

Jeong, H., Latz, M., 1994. Growth and grazing rates of the heterotrophic dinoflagellates Protoperidinium spp. on red tide dinoflagellates. Mar. Ecol. Prog. Ser. 106, 173–185 https://doi.org/10.3354/meps106173.

Jeong, H.J., 1994. Predation by the heterotrophic dinoflagellate Protoperidinium cf. divergens on copepod eggs and early naupliar stages. Mar. Ecol. Prog. Ser. 114, 203–203.

Jeong, H.J., Yoo, Y.D., Kim, J.S., Seong, K.A., Kang, N.S., Kim, T.H., 2010. Growth, feeding and ecological roles of the mixotrophic and heterotrophic dinoflagellates in marine planktonic food webs. Ocean Sci. J. 45, 65–91 https://doi.org/10.1007/s12601-010-0007-2.

Kemp, A.E.S., Villareal, T.A., 2018. The case of the diatoms and the muddled mandalas: time to recognize diatom adaptations to stratified waters. Prog. Oceanogr. 167, 138–149 https://doi.org/10.1016/j.pocean.2018.08.002.

Killick, R., Eckley, I.A., 2014. changepoint : an R Package for Changepoint Analysis. J. Stat. Softw. 58, 1–19 https://doi.org/10.18637/jss.v058.i03.

Kim, S., Kang, Y., Kim, H., Yih, W., Coats, D., Park, M., 2008. Growth and grazing responses of the mixotrophic dinoflagellate Dinophysis acuminata as functions of light intensity and prey concentration. Aquat. Microb. Ecol. 51, 301–310 https://doi.org/10.3354/ame01203.

Lee, K.H., Jeong, H.J., Yoon, E.Y., Jang, S.H., Kim, H.S., Yih, W., 2014. Feeding by common heterotrophic dinoflagellates and a ciliate on the red-tide ciliate Mesodinium rubrum. ALGAE 29, 153–163 https://doi.org/10.4490/algae.2014.29.2.153.

Legendre, P., Borcard, D., 2018. Box-Cox-chord transformations for community composition data prior to beta diversity analysis. Ecography https://doi.org/10.1111/ecog.03498.

Legendre, P., Dallot, S., Legendre, L., 1985. Succession of species within a community: chronological clustering, with applications to marine and freshwater zooplankton. Am. Nat. 125, 257–288.

Legendre, P., Gallagher, E., 2001. Ecologically meaningful transformations for ordination of species data. Oecologia 129, 271–280 https://doi.org/10.1007/s004420100716.

Litchman, E., Klausmeier, C.A., Schofield, O.M., Falkowski, P.G., 2007. The role of functional traits and trade-offs in structuring phytoplankton communities: scaling from cellular to ecosystem level. Ecol. Lett. 10, 1170–1181 https://doi.org/10.1111/j.1461-0248.2007.01117.x.

López-Urrutia, , San Martin, E., Harris, R.P., Irigoien, X., 2006. Scaling the metabolic balance of the oceans. Proc. Natl. Acad. Sci. Unit. States Am. 103, 8739–8744.

Lund, J.W.G., Kipling, C., Le Cren, E.D., 1958. The inverted microscope method of estimating algal numbers and the statistical basis of estimations by counting. Hydrobiologia 11, 143–170.

Marañón, E., 2015. Cell size as a key determinant of phytoplankton metabolism and community structure. Annu. Rev. Mar. Sci. 7, 241–264 https://doi.org/10.1146/annurev-marine-010814-015955.

Margalef, R., 1978. Life-forms of phytoplankton as survival alternatives in an unstable environment. Oceanol. Acta 1, 493–509.

Margalef, R., 1963. Succession in marine populations. Adv. Front. Plant Sci. 137–188.

Marty, J.C., Chiavérini, J., 2010. Hydrological changes in the Ligurian Sea (NW Mediterranean, DYFAMED site) during 1995–2007 and biogeochemical consequences. Biogeosciences 7, 2117–2128 https://doi.org/10.5194/bg-7-2117-2010.

Mazzocchi, M.G., Christou, E.D., Capua, I.D., Fernández de Puelles, M., Fonda-Umani, S., Molinero, J.C., Nival, P., Siokou-Frangou, I., 2007. Temporal variability of Centropages typicus in the Mediterranean Sea over seasonal-to-decadal scales. Prog. Oceanogr. 72, 214–232 https://doi.org/10.1016/j.pocean.2007.01.004.

McGill, B., Enquist, B., Weiher, E., Westoby, M., 2006. Rebuilding community ecology from functional traits. Trends Ecol. Evol. 21, 178–185 https://doi.org/10.1016/j.tree.2006.02.002.

Mitra, A., Flynn, K.J., 2010. Modelling mixotrophy in harmful algal blooms: more or less the sum of the parts?. J. Mar. Syst. 83, 158–169 https://doi.org/10.1016/j.jmarsys.2010.04.006.

Mohamed, Z.A., 2018. Potentially harmful microalgae and algal blooms in the Red Sea: current knowledge and research needs. Mar. Environ. Res. https://doi.org/10.1016/j.marenvres.2018.06.019.

Murphy, J., Riley, J.P., 1962. A modified single solution method for the determination of phosphate in natural waters. Anal. Chim. Acta 31–36.

Nair, A., Sathyendranath, S., Platt, T., Morales, J., Stuart, V., Forget, M.-H., Devred, E., Bouman, H., 2008. Remote sensing of phytoplankton functional types. Remote Sens. Environ. 112, 3366–3375 https://doi.org/10.1016/j.rse.2008.01.021.

Naselli-Flores, L., Padisák, J., Albay, M., 2007. Shape and size in phytoplankton ecology: do they matter?. Hydrobiologia 578, 157–161 https://doi.org/10.1007/s10750-006-2815-z.

Nicolau, R., Galera-Cunha, A., Lucas, Y., 2006. Transfer of nutrients and labile metals from the continent to the sea by a small Mediterranean river. Chemosphere 63, 469–476 https://doi.org/10.1016/j.chemosphere.2005.08.025.

Nicolau, R., Lucas, Y., Merdy, P., Raynaud, M., 2012. Base flow and stormwater net fluxes of carbon and trace metals to the Mediterranean sea by an urbanized small river. Water Res. 46, 6625–6637 https://doi.org/10.1016/j.watres.2012.01.031.

Novarino, G., Mills, D.K., Hannah, F., 1997. Pelagic flagellate populations in the southern North Sea, 1988-89. L Qualitative observations. J. Plankton Res. 29.

Nunes, S., Latasa, M., Gasol, J., Estrada, M., 2018. Seasonal and interannual variability of phytoplankton community structure in a Mediterranean coastal site. Mar. Ecol. Prog. Ser. 592, 57–75 https://doi.org/10.3354/meps12493.

Olenina, I., Hajdu, S., Edler, L., Andersson, A., Wasmund, N., Busch, S., Göbel, J., Gromisz, S., Huseby, S., Huttunen, M., Jaanus, A., Kokkonen, P., Ledaine, I., Niemkiewicz, E., 2006. Biovolumes and size-classes of phytoplankton in the Baltic Sea. HELCOM Balt. Sea Environ. Proc. 114pp.

Olli, K., Clarke, A., Danielsson, , Aigars, J., Conley, D.J., Tamminen, T., 2008. Diatom stratigraphy and long-term dissolved silica concentrations in the Baltic Sea. J. Mar. Syst. 73, 284–299 https://doi.org/10.1016/j.jmarsys.2007.04.009.

O'Reilly, J.E., Maritorena, S., Mitchell, B.G., Siegel, D.A., Carder, K.L., Garver, S.A., Kahru, M., McClain, C., 1998. Ocean color chlorophyll algorithms for SeaWiFS. J. Geophys. Res. Oceans 103, 24937–24953 https://doi.org/10.1029/98JC02160.

Park, M.G., Kim, M., Kang, M., 2013. A dinoflagellate Amylax triacantha with plastids of the cryptophyte origin: phylogeny, feeding mechanism, and growth and grazing responses. J. Eukaryot. Microbiol. 60, 363–376 https://doi.org/10.1111/jeu.12041.

Pasqueron de Fommervault, O., Migon, C., D´Ortenzio, F., Ribera d'Alcalà, M., Coppola, L., 2015. Temporal variability of nutrient concentrations in the northwestern Mediterranean sea (DYFAMED time-series station). Deep-Sea Res. Part A Oceanogr. Res. Pap. 100, 1–12 https://doi.org/10.1016/j.dsr.2015.02.006.

Pougnet, F., Schäfer, J., Dutruch, L., Garnier, C., Tessier, E., Dang, D.H., Lanceleur, L., Mullot, J.-U., Lenoble, V., Blanc, G., 2014. Sources and historical record of tin and butyl-tin species in a Mediterranean bay (Toulon Bay, France). Environ. Sci. Pollut. Res. 21, 6640–6651 https://doi.org/10.1007/s11356-014-2576-6.

Redfield, A.C., Ketchum, B.H., Richards, F.A., 1963. The influence of organims on the composition of sea-water. In: The Influence of Organisms on the Composition of Seawater, the Sea. Hill MN, pp. 26–77.

Reynolds, C.S., 2006. Ecology of Phytoplankton. Cambridge University Press, Cambridge; New York.

Richard, S., Jamet, J.-L., 2001. An unusual distribution of Oithona nana Griesbrecht (1892) (Crustacea: cyclopoida) in a bay: the case of Toulon bay (France, Mediterranean sea). J. Coast. Res. 17, 957–963.

Root, R.B., 1967. The niche exploitation pattern of the blue-gray gnatcatcher. Ecol. Monogr. 37, 317–350 https://doi.org/10.2307/1942327.

Rossi, Jamet, 2009. Structure and succession of plankton communities in two mediterranean neighbouring coastal ecosystems (Toulon bays, France). In: New Oceanography Research Development. Nova Science Publishers, pp. 1–14.

Saad, J.F., Unrein, F., Tribelli, P.M., López, N., Izaguirre, I., 2016. Influence of lake trophic conditions on the dominant mixotrophic algal assemblages. J. Plankton Res. https://doi.org/10.1093/plankt/fbw029.

Sakka, A., Legendre, L., Gosselin, M., Delesalle, B., 2000. Structure of the oligotrophic planktonic food web under low grazing of heterotrophic bacteria:Takapoto Atoll, French Polynesia. Mar. Ecol. Prog. Ser. 197, 1–17 https://doi.org/10.3354/meps197001.

Sammari, C., Millot, C., Prieur, L., 1995. Aspects of the seasonal and mesoscale variabilities of the Nothern current in the western Mediterranean Sea inferred from the PROLIG-2 and PROS-6 experiments. Deep Sea Res. Part I 42, 893–917.

Serranito, B., Aubert, A., Stemmann, L., Rossi, N., Jamet, J.L., 2016. Proposition of indicators of anthropogenic pressure in the Bay of Toulon (Mediterranean Sea) based on zooplankton time-series. Cont. Shelf Res. 121, 3–12 https://doi.org/10.1016/j.csr.2016.01.016.

Shim, J.-B., Klochkova, T.A., Han, J.-W., Kim, G.-H., Yoo, Y.-D., Jeong, H.-J., 2011. Comparative proteomics of the mixotrophic dinoflagellate Prorocentrum micans growing in different trophic modes. ALGAE 26, 87–96 https://doi.org/10.4490/algae.2011.26.1.087.

Sieburth, J.M., Smetacek, V., Lenz, J., 1978. Pelagic ecosystem structure: heterotrophic compartiments of the plankton and their relationship to plankton size fractions. Limnol. Oceanogr. 23 (6), 1256–1263.

Siokou-Frangou, I., Christaki, U., Mazzocchi, M.G., Montresor, M., Ribera d'Alcalá, M., Vaqué, D., Zingone, A., 2010. Plankton in the open Mediterranean sea: a review. Biogeosciences 7, 1543–1586 https://doi.org/10.5194/bg-7-1543-2010.

Skejić, S., Car, A., Marasović, I., Jozic, S., Bužančić, M., Arapov, J., Ninčević Gladan, , Bakrac, A., Kušpilić, G., Vidjak, O., Larsen, J., 2017. Morphology and ecology of the poorly known dinoflagellate prorocentrum arcuatum (dinophyceae) from the medulin bay (eastern Adriatic sea). Acta Adriat. 58, 41–52.

Smalley, G., Coats, D., Stoecker, D., 2003. Feeding in the mixotrophic dinoflagellate Ceratium furca is influenced by intracellular nutrient concentrations. Mar. Ecol. Prog. Ser. 262, 137–151 https://doi.org/10.3354/meps262137.

Smalley, G.W., Coats, D.W., 2002. Ecology of the red-tide dinoflagellate ceratium furca: distribution, mixotrophy, and grazing impact on ciliate populations of chesapeake bay. J. Eukaryot. Microbiol. 49, 63–73 https://doi.org/10.1111/j.1550-7408.2002.tb00343.x.

Smayda, T.J., Reynolds, C.S., 2003. Strategies of marine dinoflagellate survival and some rules of assembly. J. Sea Res. 49, 95–106 https://doi.org/10.1016/S1385-1101(02)00219-8.

Smayda, T.J., Reynolds, C.S., 2001. Community assembly in marine phytoplankton: application of recent models to harmful dinoflagellate blooms. J. Plankton Res. 23, 447–461.

Smetacek, V., Cloern, J.E., 2008. OCEANS: on phytoplankton trends. Science 319, 1346–1348 https://doi.org/10.1126/science.1151330.

Somot, S., Sevault, F., Déqué, M., 2006. Transient climate change scenario simulation of the Mediterranean Sea for the twenty-first century using a high-resolution ocean circulation model. Clim. Dyn. 27, 851–879 https://doi.org/10.1007/s00382-006-0167-z.

Spilling, K., Olli, K., Lehtoranta, J., Kremp, A., Tedesco, L., Tamelander, T., Klais, R., Peltonen, H., Tamminen, T., 2018. Shifting diatom—dinoflagellate dominance during spring bloom in the Baltic Sea and its potential effects on biogeochemical cycling. Front. Mar. Sci. 5, 327 https://doi.org/10.3389/fmars.2018.00327.

Stoecker, D.K., 1999. Mixotrophy among Dinoflagellates1. J. Eukaryot. Microbiol. 46, 397–401 https://doi.org/10.1111/j.1550-7408.1999.tb04619.x.

Strickland, J.D.H., Parsons, T.R., 1968. A practical handbook of seawater analysis - determination of reactive phosphorus. In: Journal of the Fisheries Research Board of Canada. pp. 49–56.

Sun, J., Liu, D., 2003. Geometric models for calculating cell biovolume and surface area for phytoplankton. J. Plankton Res. 25, 1331–1346 https://doi.org/10.1093/plankt/fbg096.

Taupier-Letage, I., Millot, C., 1986. General hydrodynamical features in the Ligurian Sea inferred from the DYOME experiment. Oceanol. Acta 9, 119–131.

Taupier-Letage, I., Piazzola, J., Zakardjian, B., 2013. Les îles d'Hyères dans le système de circulation marine et atmosphérique de la Méditerranée. Sci. Rep. Port-Cros Natl. Park 27, 29–52.

Tessier, E., Garnier, C., Mullot, J.-U., Lenoble, V., Arnaud, M., Raynaud, M., Mounier, S., 2011. Study of the spatial and historical distribution of sediment inorganic contamination in the Toulon bay (France). Mar. Pollut. Bull. 62, 2075–2086 https://doi.org/10.1016/j.marpolbul.2011.07.022.

Tett, P., Carreira, C., Mills, D.K., Van Leeuwen, S., Foden, J., Bresnan, E., Gowen, R.J., 2008. Use of a Phytoplankton Community Index to assess the health of coastal waters. ICES J. Mar. Sci. J. Cons. 65, 1475–1482.

Tett, P., Gowen, R., Mills, D., Fernandes, T., Gilpin, L., Huxham, M., Kennington, K., Read, P., Service, M., Wilkinson, M., Malcolm, S., 2007. Defining and detecting undesirable disturbance in the context of marine eutrophication. Mar. Pollut. Bull. 55, 282–297 https://doi.org/10.1016/j.marpolbul.2006.08.028.

Tett, P., Gowen, R., Painting, S., Elliott, M., Forster, R., Mills, D., Bresnan, E., Capuzzo, E., Fernandes, T., Foden, J., Geider, R., Gilpin, L., Huxham, M., McQuatters-Gollop, A., Malcolm, S., Saux-Picart, S., Platt, T., Racault, M., Sathyendranath, S., van der Molen, J., Wilkinson, M., 2013. Framework for understanding marine ecosystem health. Mar. Ecol. Prog. Ser. 494, 1–27 https://doi.org/10.3354/meps10539.

Totti, C., Romagnoli, T., Accoroni, S., Coluccelli, A., Pellegrini, M., Campanelli, A., Grilli, F., Marini, M., 2019. Phytoplankton communities in the northwestern Adriatic Sea: interdecadal variability over a 30-years period (1988–2016) and relationships with meteoclimatic drivers. J. Mar. Syst. 193, 137–153 https://doi.org/10.1016/j.jmarsys.2019.01.007.

Tréguer, P., Le Corre, P., 1975. Manuel d'analyse des sels nutritifs dans l'eau de mer (utilisation de l'AutoAnalyser II Technicon (r)). In: Brest: Université de Bretagne Occidentale, 2ème édition.

Trigo, I.F., Davies, T.D., 2000. Decline in Mediterranean rainfall caused by weakening of Mediterranean cyclones. Geophys. Res. Lett. 27, 2913–2916.

Uitz, J., Stramski, D., Gentili, B., D'Ortenzio, F., Claustre, H., 2012. Estimates of phytoplankton class-specific and total primary production in the Mediterranean Sea from satellite ocean color observations: PRIMARY PRODUCTION IN THE MEDITERRANEAN. Glob. Biogeochem. Cycles 26, 1–10 https://doi.org/10.1029/2011GB004055.

Utermöhl, H., 1958. Zur Vervollkommnung der quantitativen Phytoplankton-Methodik. Mitt. Int. Ver. Fuer Theor. Unde Amgewandte Limnol. 1–38.

Vadrucci, M.R., Cabrini, M., Basset, A., 2007. Biovolume determination of phytoplankton guilds in transitional water ecosystems of Mediterranean Ecoregion. Transitional Waters Bull 83–102.

Vadrucci, M.R., Mazziotti, C., Fiocca, A., 2013. Cell biovolume and surface area in phytoplankton of Mediterranean transitional water ecosystems: methodological aspects. Transitional Waters Bull 7, 100–123.

Vargas-Yáñez, M., Jesús García, M., Salat, J., García-Martínez, M.C., Pascual, J., Moya, F., 2008. Warming trends and decadal variability in the Western Mediterranean shelf. Glob. Planet. Chang. 63, 177–184 https://doi.org/10.1016/j.gloplacha.2007.09.001.

Vargas-Yáñez, M., Moya, F., García-Martínez, M.C., Tel, E., Zunino, P., Plaza, F., Salat, J., Pascual, J., López-Jurado, J.L., Serra, M., 2010. Climate change in the western Mediterranean sea 1900–2008. J. Mar. Syst. 82, 171–176 https://doi.org/10.1016/j.jmarsys.2010.04.013.

Vila, M., Maso, M., 2005. Phytoplankton functional groups and harmful algal species in anthropogenically impacted waters of the NW Mediterranean Sea. Sci. Mar. 69, 31–45.

Wang, S., Maltrud, M.E., Burrows, S.M., Elliott, S.M., Cameron-Smith, P., 2018. Impacts of shifts in phytoplankton community on clouds and climate via the sulfur cycle. Glob. Biogeochem. Cycles 32, 1005–1026 https://doi.org/10.1029/2017GB005862.

Ward, B.A., Follows, M.J., 2016. Marine mixotrophy increases trophic transfer efficiency, mean organism size, and vertical carbon flux. Proc. Natl. Acad. Sci. Unit. States Am. 113, 2958–2963 https://doi.org/10.1073/pnas.1517118113.

Weithoff, G., Beisner, B.E., 2019. Measures and approaches in trait-based phytoplankton community ecology – from freshwater to marine ecosystems. Front. Mar. Sci. 6, https://doi.org/10.3389/fmars.2019.00040.

Weithoff, G., Wacker, A., 2007. The mode of nutrition of mixotrophic flagellates determines the food quality for their consumers. Funct. Ecol. 21, 1092–1098 https://doi.org/10.1111/j.1365-2435.2007.01333.x.

Yamaguchi, A., Horiguchi, T., 2005. Molecular phylogenetic study of the heterotrophic dinoflagellate genus Protoperidinium (Dinophyceae) inferred from small subunit rRNA gene sequences. Phycol. Res. 53, 30–42 https://doi.org/10.1111/j.1440-183.2005.00370.x.

Yoo, Y.D., Jeong, H.J., Kang, N.S., Song, J.Y., Kim, K.Y., Lee, G., Kim, J., 2010. Feeding by the newly described mixotrophic dinoflagellate Paragymnodinium shiwhaense: feeding mechanism, prey species, and effect of prey concentration. J. Eukaryot. Microbiol. 57, 145–158 https://doi.org/10.1111/j.1550-7408.2009.00448.x.